Article

Dietary restriction impacts health and lifespan of genetically diverse mice

https://doi.org/10.1038/s41586-024-08026-3

Received: 28 November 2023

Accepted: 5 September 2024

Published online: 9 October 2024

Open access

Check for updates

Andrea Di Francesco[1]✉, Andrew G. Deighan[2], Lev Litichevskiy[3,4], Zhenghao Chen[1], Alison Luciano[2], Laura Robinson[2], Gaven Garland[2], Hannah Donato[2], Matthew Vincent[2], Will Schott[2], Kevin M. Wright[1,6], Anil Raj[1], G. V. Prateek[1], Martin Mullis[1], Warren G. Hill[5], Mark L. Zeidel[5], Luanne L. Peters[2], Fiona Harding[1], David Botstein[1], Ron Korstanje[2], Christoph A. Thaiss[3], Adam Freund[1,7] & Gary A. Churchill[2]✉

Caloric restriction extends healthy lifespan in multiple species[1]. Intermittent fasting, an alternative form of dietary restriction, is potentially more sustainable in humans, but its effectiveness remains largely unexplored[2–8]. Identifying the most efficacious forms of dietary restriction is key for developing interventions to improve human health and longevity[9]. Here we performed an extensive assessment of graded levels of caloric restriction (20% and 40%) and intermittent fasting (1 and 2 days fasting per week) on the health and survival of 960 genetically diverse female mice. We show that caloric restriction and intermittent fasting both resulted in lifespan extension in proportion to the degree of restriction. Lifespan was heritable and genetics had a larger influence on lifespan than dietary restriction. The strongest trait associations with lifespan included retention of body weight through periods of handling—an indicator of stress resilience, high lymphocyte proportion, low red blood cell distribution width and high adiposity in late life. Health effects differed between interventions and exhibited inconsistent relationships with lifespan extension. 40% caloric restriction had the strongest lifespan extension effect but led to a loss of lean mass and changes in the immune repertoire that could confer susceptibility to infections. Intermittent fasting did not extend the lifespan of mice with high pre-intervention body weight, and two-day intermittent fasting was associated with disruption of erythroid cell populations. Metabolic responses to dietary restriction, including reduced adiposity and lower fasting glucose, were not associated with increased lifespan, suggesting that dietary restriction does more than just counteract the negative effects of obesity. Our findings indicate that improving health and extending lifespan are not synonymous and raise questions about which end points are the most relevant for evaluating aging interventions in preclinical models and clinical trials.

Caloric restriction (CR) delays the onset of age-related diseases and extends lifespan in multiple species[1]. In humans, compliance with CR is challenging, and interest has shifted to more permissive forms of dietary restriction (DR), such as time-restricted feeding and intermittent fasting (IF) that have proven to be effective in promoting organismal health[2–5]. In mice, regular periods of fasting can convey considerable benefits without reduction in overall energy intake[6]. Mice on CR also experience prolonged periods of daily fasting, and the health benefits of CR can be optimized by feeding at a specific time of the day, suggesting that both caloric intake and timing of feeding contribute to physiological response and lifespan extension[5–8]. Despite the importance of these observations, limited information is available regarding the differences between CR and IF in relation to healthy ageing and longevity[9].

Responses to DR vary across individuals, and the mechanisms underlying this variability remain largely unclear. Studies in mice and non-human primates have shown that the effects of DR are influenced by individual characteristics including sex, body size and composition, and genetics[10–17]. Human clinical studies testing the effects of DR on health have largely focused on changes in body weight, adiposity, energy metabolism and cardiometabolic risk factors[18–23]. There has been less exploration of the long-term effects of DR because studies in humans are limited by their small sample size and short duration. Moreover, the safety and efficacy of DR may depend on factors such

[1]Calico Life Sciences LLC, South San Francisco, CA, USA. [2]The Jackson Laboratory, Bar Harbor, ME, USA. [3]Department of Microbiology, Perelman School of Medicine, University of Pennsylvania, Philadelphia, PA, USA. [4]Department of Biostatistics, Epidemiology and Informatics, Perelman School of Medicine, University of Pennsylvania, Philadelphia, PA, USA. [5]Division of Nephrology, Department of Medicine, Beth Israel Deaconess Medical Center and Harvard Medical School, Boston, MA, USA. [6]Present address: Actio Biosciences, San Diego, CA, USA. [7]Present address: Arda Therapeutics, San Carlos, CA, USA. ✉e-mail: andrea@calicolabs.com; gary.churchill@jax.org

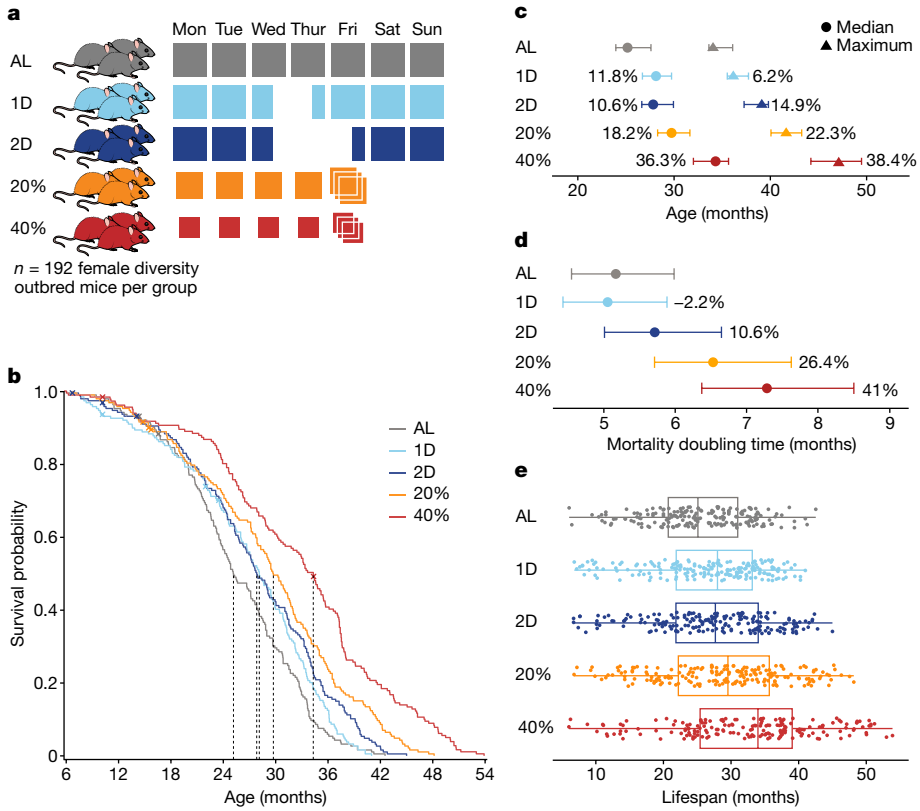

Fig. 1 | DR extends lifespan in DO mice. a, The study design: 960 female DO mice were randomized to one of five diet intervention groups: ad libitum (AL); one day (1D) or two consecutive days (2D) per week fasting; or CR at 20% (20%) or 40% (40%) of estimated adult food intake. **b**, Kaplan–Meier survival curves by diet group. The dashed lines indicate the median lifespan. Censoring events are indicated by an 'X'. **c**, Kaplan–Meier estimates of median (50% mortality) and maximum (90% mortality) lifespan by diet group, showing the percentage change relative to AL and the 95% confidence intervals (computed using R/survfit). $n = 937$ mice. **d**, Mortality doubling times estimated from a Gompertz log-linear hazard model, showing the percentage change relative to AL and the 95% confidence intervals (computed using R/flexsurvreg). $n = 937$ mice. **e**, Individual mouse lifespans (points) within diet groups. $n = 188$ (AL), $n = 188$ (1D), $n = 190$ (2D), $n = 189$ (20%) and $n = 182$ (40%). The box plots show the median lifespan (centre line), quartiles (box limits) and range (whiskers).

as age and health condition[24]. There is a lack of knowledge regarding physiological markers that predict how individuals will respond to DR. Identification of such predictors could help to tailor DR to individual needs, serve as tools in the longitudinal evaluation of intervention success and elucidate the biological processes that mediate the effects of DR on lifespan.

In this study of dietary restriction in diversity outbred mice (DRiDO), we investigated the effects of CR and IF on the health and lifespan of female diversity outbred (DO) mice[25]. In addition to measuring lifespan, we performed hundreds of longitudinal assessments to evaluate the health effects of DR. Recent studies using UM-HET3 mice, another genetically diverse mouse population, have revealed genetic variants associated with normative ageing[26]. We used DO mice because findings in genetically diverse mice are more likely to generalize across species, and because DO mice present a wide range of physiological characteristics, including variation in body composition and other metabolic traits[27], that could serve as predictive markers of individual response to DR. The goals of our study were (1) to characterize the lifespan and health effects of DR; and (2) to identify physiological and genetic factors that predict individual responses to DR.

DR extends lifespan in female DO mice

We examined the effects of graded levels of CR and IF on 960 female DO mice that were randomly assigned to one of five diets: ad libitum feeding (AL), fasting one day per week (1D group) or two consecutive days per week (2D group), and CR at 20% or 40% of baseline ad libitum food intake (Fig. 1a). At 6 months of age, we initiated DR on 937 surviving mice and maintained them on DR for the duration of their natural lifespan.

We used an additional 160 DO mice to evaluate daily and cumulative food intake (Extended Data Fig. 1a–c). IF mice had their food removed at 15:00 on Wednesday and replenished after 24 h (1D group) or 48 h (2D group) (Fig. 1a). These mice displayed compensatory feeding after the fasting period such that cumulatively 1D mice consumed a similar amount of food to AL mice, and 2D mice consumed 12% less food than AL mice (Extended Data Fig. 1b,c). Over the fasting period, 1D and 2D IF mice lost and later recovered an average of 2.5 g and 4.0 g body weight, respectively (Extended Data Fig. 1d). CR mice were fed a measured amount of food daily at 15:00. On Friday afternoon, CR mice received a triple allotment of food that was typically consumed by 15:00 on Saturday (40% CR) or 15:00 on Sunday (20% CR), resulting in weekly fasting periods like those experienced by IF mice (Extended Data Fig. 1a). The CR mice showed less than 1 g average change in body weight over the weekend despite experiencing a period of fasting.

At ages of around 5, 16 and 26 months, the mice in the main study cohort were monitored in metabolic cages to observe how DR affected daily fluctuations in food consumption, respiratory quotient (a measure of metabolic substrate usage), energy expenditure) and wheel running activity (Extended Data Fig. 2a–d). All groups of mice began daily feeding just before lights-off (Extended Data Fig. 2a), but CR mice consumed the available food within a few hours, resulting in extended periods of daily fasting. Daily and weekly fluctuations in respiratory quotient tracked the fed and fasted states and were most pronounced in the 40% CR group (Extended Data Fig. 2e). Energy expenditure adjusted for body weight was lowest in the 40% CR group, followed by the 20%

CR and 2D IF groups (Extended Data Fig. 2f). Wheel running activity decreased with age, except for the 40% CR mice, which showed the highest cumulative wheel running (Extended Data Fig. 2g), including a mid-day wheel running bout consistent with food-seeking behaviour[28,29] (Extended Data Fig. 2d).

DR extended the lifespan of female DO mice (log-rank $P < 2.2 \times 10^{-16}$), with responses proportional to the degree of restriction or length of fasting (40% > 20% > 2D > 1D > AL; Fig. 1b and Supplementary Table 1). DR affected both the median and maximum lifespan (Kaplan–Meier estimates of 50% and 90% mortality, respectively[30]; Fig. 1c and Supplementary Table 2). 40% CR mice achieved a median lifespan of around 9 months (36.3%) greater than mice in the AL group. Notably, IF mice experienced an extended median lifespan with minimal or no reduction in net caloric intake. We estimated the mortality doubling time by fitting Gompertzian lifespan models[31] to the post-DR survival data (Fig. 1d and Supplementary Table 3) and observed a significant decrease in the rate of ageing for CR mice but not for IF mice compared with AL mice (overall diet effect on Gompertz model slope, $P = 7.78 \times 10^{-4}$).

Despite the profound effects of DR, lifespan was highly variable within diet groups (Fig. 1e). This led us to examine whether any physiological traits could explain the variability in lifespan. We evaluated more than 200 traits across 12 groups of assays repeated across time (Extended Data Fig. 3a), resulting in up to 724 measurements per mouse. We obtained weekly body weights; assessed frailty index, grip strength and body temperature every 6 months; and performed yearly assessments, including metabolic cage analysis, body composition, echocardiogram, wheel running, rotarod, acoustic startle, bladder function, fasting glucose, immune cell profiling and whole-blood analysis (see the 'Phenotyping' section of the Methods; Supplementary Tables 4 and 5). We performed longitudinal analyses to assess which traits were influenced by body weight, age and diet (Extended Data Fig. 3b and Supplementary Table 6). We performed linear regression analysis to identify which traits were associated with lifespan after accounting for diet and body weight (Extended Data Fig. 3c–e and Supplementary Table 7). In the following sections, we examine the effects of diets on body weight and composition; we then look at the effects of DR on indicators of health, including metabolic, immune and haematological traits; and, finally, we examine the effects of genetics on health and lifespan.

Impact of DR on body weight and composition

DR substantially altered lifetime body weight trajectories (Fig. 2a and Extended Data Fig. 4a). Weight loss on DR was approximately proportional to the degree of CR, but there was an additional effect of IF on body weight, for example, 1D mice showed reduced body weight relative to AL mice despite having a similar caloric intake (Extended Data Fig. 1c). The 40% CR mice showed rapid body weight decline at the onset of DR and lost an average of 24.3% of their 6-month-old body weight by 18 months of age. By contrast, AL mice gained an average of 28.4% body weight over the same period. Weight loss in the 40% CR mice persisted throughout life, suggesting that most of these animals never achieved energy balance. Rescaling chronological age to proportion of life lived (PLL = age at test/lifespan) enabled us to better compare traits near the end-of-life without distortion by differential survivorship (Fig. 2b). For all mice except for the 40% CR group, average weight gain continued through midlife, stabilized between 0.50 to 0.75 PLL, and declined rapidly near the end of life (beyond 0.90 PLL). End-of-life weight loss may reflect the presence of cancer or other terminal disease, but we were unable to determine the cause of death for most mice.

High early body weight has been associated with reduced lifespan in mice and other species[32–34]. Consistent with these findings, we observed a negative diet-adjusted association between lifespan and pre-intervention bodyweight (Fig. 2c (top row) and Extended Data Fig. 4b). However, this negative association weakened with age and became positive beyond 2 years (Fig. 2c (top row) and Extended Data Fig. 4c). For 2D IF mice, a difference of 1 g in body weight at 2 months of age corresponded to a reduction in expected in lifespan of 0.66 months (20 days), but this association weakened with age (Fig. 2d). The reversal of the body-weight–lifespan association with age was present in all diet groups. We next examined whether early body weight might also modify response to DR. Kaplan–Meier analysis stratified by the median 6-month body weight showed that CR extended lifespan to the same extent in lighter and heavier mice (Fig. 2e, Extended Data Fig. 4d and Supplementary Table 8). By contrast, IF mice with high pre-intervention body weight showed no evidence of extended lifespan.

Moreover, we assessed whether individual lifespan extension could be explained by changes in body weight in the post-DR period. Notably, we found that, within diet groups, mice that retained more weight had longer lifespans[35] (Extended Data Fig. 4e). In contrast to the conventional notion suggesting that the beneficial effects of DR are due to reduced levels of obesity[36], body weight loss at any age was associated with reduced lifespan (Fig. 2c (second row)). These results argue against the notion that DR works simply by counteracting the negative effects of obesity.

During the one-month-long phenotyping periods at 10, 22 and 34 months of age, mice experienced stress due to handling, resulting in short-term weight loss followed by recovery in the following weeks. Change in body weight across the phenotyping period from 10 to 11 months of age (PhenoDelta) showed the strongest association with lifespan across all traits examined in this study (Fig. 2f and Extended Data Fig. 3d). Mice that were most resilient to weight loss had a longer lifespan. Weight loss during the 22-month-old phenotyping period was also associated with reduced lifespan (Extended Data Fig. 4f).

We analysed body composition at 10, 22 and 34 months of age to obtain fat tissue mass (FTM) and lean tissue mass (LTM), and we also calculated the total tissue mass (TTM = FTM + LTM) and adiposity (percentage fat = FTM/TTM). The genetically diverse mice displayed wide variation in body weight and composition, with adiposity ranging from less than 10% to over 60% across all diet groups and ages (Extended Data Fig. 5a). For AL and IF mice, LTM increased throughout life (Fig. 2h). For CR mice, LTM was substantially reduced compared with in AL mice over the 4-month post-intervention period and remained constant (20% CR) or declined (40% CR) with age. All groups of mice lost fat mass with age, particularly in the latter half of life (Fig. 2i). While 40% CR mice had the lowest average adiposity, 20% CR mice had adiposity levels comparable to AL mice, and individual mice with the highest adiposity were found in the 20% CR group (Extended Data Fig. 5a).

Previous studies have shown that preserving adiposity may increase survival in response to chronic CR[11,16,37]. We examined the association between lifespan and adiposity at 10 and 22 months of age (Extended Data Fig. 5b,c). Higher adiposity was generally associated with increased lifespan. This association was stronger in older mice subjected to either 2D IF or CR. Among all of the traits that we tested for association with lifespan, only TTM and LTM at 10 months of age indicated significant diet-specific associations with lifespan (diet × trait: $P_{adj} < 0.01$) and FTM at 10 months was nearly significant (Extended Data Fig. 5d,e). Specifically, higher LTM was associated with a shorter lifespan in IF mice but a longer lifespan in 40% CR mice. Collectively, these results highlight a paradox: DR extends lifespan while decreasing body weight and fat mass, yet preserving body weight and fat mass is associated with longer lifespan. This paradox is a recurrent theme in this study.

Impact of DR on health and metabolism

Most of the health-related traits in our phenotyping pipeline changed with age and many responded to DR (Extended Data Fig. 3b), but surprisingly few of these traits showed associations with lifespan (Fig. 3a,b and Extended Data Fig. 3c). One exception was the 28-month frailty index[38] (FI; Fig. 3c,d), an indicator of morbidity that measures age-related

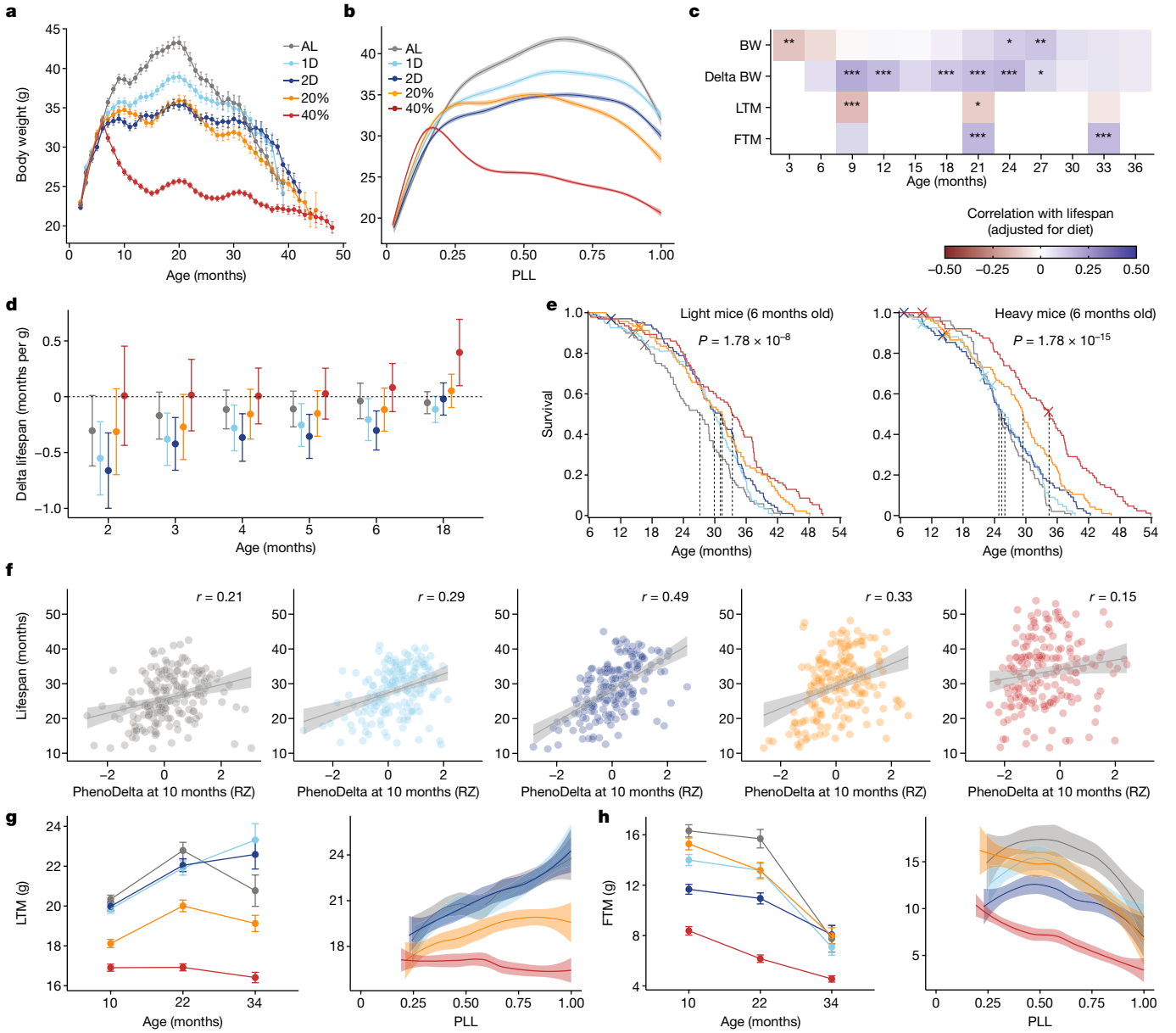

Fig. 2 | Body weight and composition effects on lifespan. a, Lifetime trajectories of body weight (g) by diet groups. Data are monthly mean ± 1 s.e.m. $n = 937$. **b**, Body weight (g) trajectories as the running median (loess fit) by the PLL with 95% confidence bands. **c**, Diet-adjusted correlation with lifespan for body weight, change in body weight across three-month intervals (delta BW), LTM and FTM. The asterisks indicate multiple-testing-adjusted significance, determined by linear regression of lifespan on traits; $^{*}P_{adj} < 0.01$, $^{**}P_{adj} < 0.001$, $^{***}P_{adj} < 0.0001$. **d**, The expected difference in lifespan per gram of body weight at ages 2 to 6 months and 18 months by diet. Data are mean ± 2 s.e.m. $n = 937$ (2 to 6 months) and $n = 802$ (18 months). **e**, Kaplan–Meier survival curves by diet group (colour) for mice below and above the median 6 month body weight. The dashed lines indicate the median survival times. Significance was determined using log-rank tests comparing diet within body weight strata. $n = 469$ (light) and $n = 468$ (heavy). **f**, Lifespan by change in body weight during the phenotyping period (10 to 11 months; PhenoDelta), showing the regression line, 95% confidence bands and diet-specific correlations ($P_{adj} < 2.2 \times 10^{-16}$; diet × trait: $P = 0.00172$, $r = 0.287$). **g**, LTM (g) by age (mean ± 2 s.e.m.; $n = 895$ (10 months), $n = 689$ (22 months), $n = 241$ (34 months) mice) and by PLL as loess smoothing with the 95% confidence band (PLL: $P < 2.2 \times 10^{-16}$; diet: $P < 2.2 \times 10^{-16}$; diet × PLL: $P = 1.07 \times 10^{-7}$). **h**, FTM (g) by age (mean ± 2 s.e.m.; n values are as shown in **g**) and by PLL as loess smoothing with the 95% confidence bands (PLL: $P < 2.2 \times 10^{-16}$, diet: $P < 2.2 \times 10^{-16}$, diet × PLL: $P = 0.168$). For **g** and **h**, details of the statistical tests are provided in the 'Longitudinal trait analysis' section of the Methods.

health deficits. Some of the frailty components most evidently affected by age included increased incidence of kyphosis and gait disorders (Extended Data Fig. 6a,b). Beneficial diet-specific responses included reduced incidence of palpable tumours and distended abdomen. We also observed that both traits were reduced in mice with a low early body weight (Extended Data Fig. 6c,d), which could contribute to the longer lifespan of these mice.

Improved glucose homeostasis, lower energy expenditure, decreased body temperature and preservation of metabolic flexibility (delta respiratory quotient) are common physiological adaptations to DR in both rodents and humans that have been suggested as potential mechanisms that mediate the extension of lifespan by DR[39,40]. Body temperature declined with age and DR (Fig. 3e). Fasting glucose was substantially reduced by DR (Fig. 3f). However, we found no significant associations between lifespan and fasting glucose, energy expenditure or delta respiratory quotient (Fig. 3b). Higher body temperature was moderately associated with increased lifespan, which was not the expected direction. Despite the profound effects of

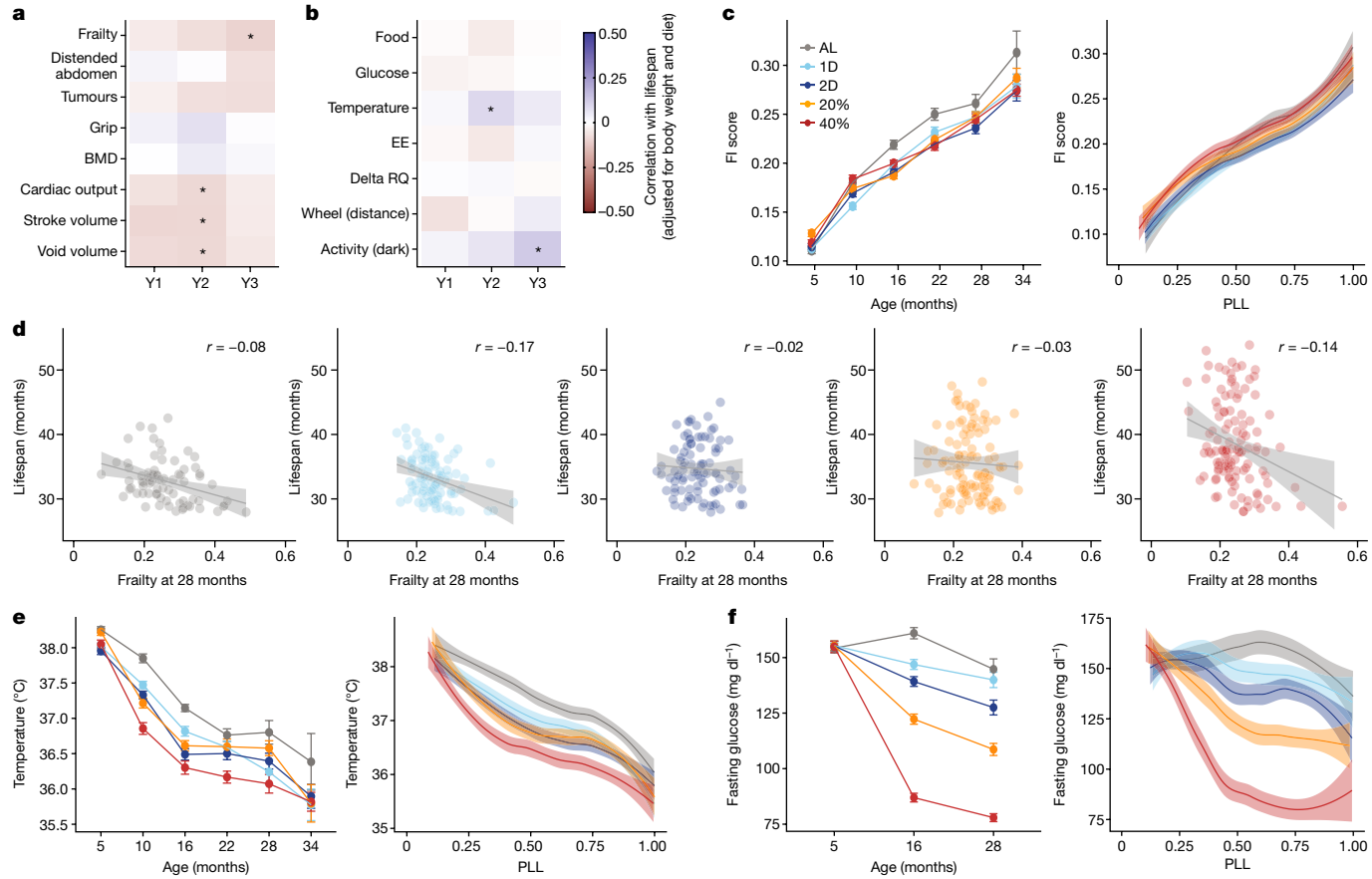

Fig. 3 | Health and metabolic traits change with age and diet but are poor predictors of lifespan. a,**b**, Heat maps of diet- and body-weight-adjusted correlation with lifespan for selected health (**a**) and metabolic (**b**) traits at annual testing intervals. Ages (1 year, 2 years and 3 years indicated as Y1, Y2 and Y3, respectively) vary depending on the assay (Supplementary Table 4). The asterisks indicate multiple-testing-adjusted significance, determined by linear regression of lifespan on traits; *$P_{adj} < 0.01$. **c**, FI score (adjusted for technician and coat colour) by age (mean ± 2 s.e.m.; $n = 770$ (5 months), $n = 909$ (10 months), $n = 834$ (16 months), $n = 704$ (22 months), $n = 489$ (28 months), $n = 260$ (34 months) mice) and by PLL as loess smoothing with the 95% confidence bands (PLL: $P < 2.2 \times 10^{-16}$; diet: $P = 7.37 \times 10^{-5}$; diet × PLL: $P = 0.633$). **d**, Lifespan by frailty score (adjusted for technician and coat colour) at 28 months with regression line and 95% confidence band ($P_{adj} = 0.00238$; diet × trait: $P = 0.260$, $r = -0.90$). **e**, Body temperature (°C; adjusted for coat colour) by age (mean ± 2 s.e.m.; sample sizes were as described in **c**) and by PLL as loess smoothing with the 95% confidence bands (PLL: $P < 2.2 \times 10^{-16}$; diet: $P < 2.2 \times 10^{-16}$; diet × PLL: $P = 0.0242$). **f**, Fasting glucose (mg dl^{-1}, adjusted for body weight) by age (mean ± 2 s.e.m.; samples sizes were as described in **c**) and by PLL as loess smoothing with the 95% confidence bands (PLL: $P < 2.80 \times 10^{-4}$; diet: $P < 2.2 \times 10^{-16}$; diet × PLL: $P = 0.0368$). Statistical details are provided in the 'Longitudinal trait analysis' (**c**,**e**,**f**) and 'Trait association with lifespan' (**d**) sections of the Methods. BMD, bone mineral density; EE, energy expenditure; RQ, respiratory quotient.

DR on metabolic traits, they displayed only weak or no associations with lifespan.

Impact of DR on blood cell populations

In contrast to health and metabolic traits, we found that many immunological and haematological traits were strongly associated with lifespan (Fig. 4a,b and Extended Data Fig. 3c). Age-related changes in immune cell subsets in DO mice were generally aligned with changes previously described in humans and in common inbred mouse strains[41–44]. Overall, the relative proportion of B cells, effector T cells and inflammatory monocytes accumulated with age, while the total fraction of lymphocytes, mature natural killer (NK) cells and eosinophils declined (Fig. 4c,d and Extended Data Fig. 7a–d). DR did not significantly modify the age-related changes in the percentage of lymphocytes or the percentage of effector T cells. However, 40% CR had a profound effect on the frequency of mature NK cells, eosinophils, circulating B cells and inflammatory monocytes (Extended Data Fig. 7a–d). The nomenclature for immune cell types is defined in Supplementary Table 9.

The percentage of total circulating lymphocytes was positively associated with lifespan (Extended Data Fig. 7e). Cells exhibiting a physiological resting state, such as $CD4^+$ and $CD8^+$ naive T cells and immature NK cells, were positively correlated with lifespan, while immune cells displaying evidence of activation or mature phenotypes, such as $CD4^+$ and $CD8^+$ effector T cells and $CD11^+$ memory B cells, were generally associated with a shortened lifespan (Extended Data Fig. 7f).

The major erythroid cell traits (haemoglobin, haematocrit, red blood cell count) decreased with age, while the red blood cell distribution width (RDW; coefficient of variation in volume of red blood cells) and the haemoglobin distribution width (HDW; coefficient of variation in erythrocyte haemoglobin concentration) both increased (Fig. 4e,g and Extended Data Fig. 7g–i). These changes co-occurred in the same animals and parallel changes were seen in ageing human populations in which anaemia is a common and substantial problem[45,46]. Haemoglobin levels were improved (increased) under CR but not under IF, suggesting a beneficial effect of CR at reducing the risk of anaemia. Diet response of RDW was distinctive. By 10 months of age, RDW was sharply increased in 2D IF mice and to a lesser extent in 40% CR mice. Many of the complete blood count (CBC) traits, including RDW and haemoglobin, showed an inflection point and higher rates of change in the last 25% of life and served as indicators of imminent mortality. Among the erythroid traits, HDW and RDW showed the strongest association with lifespan, and

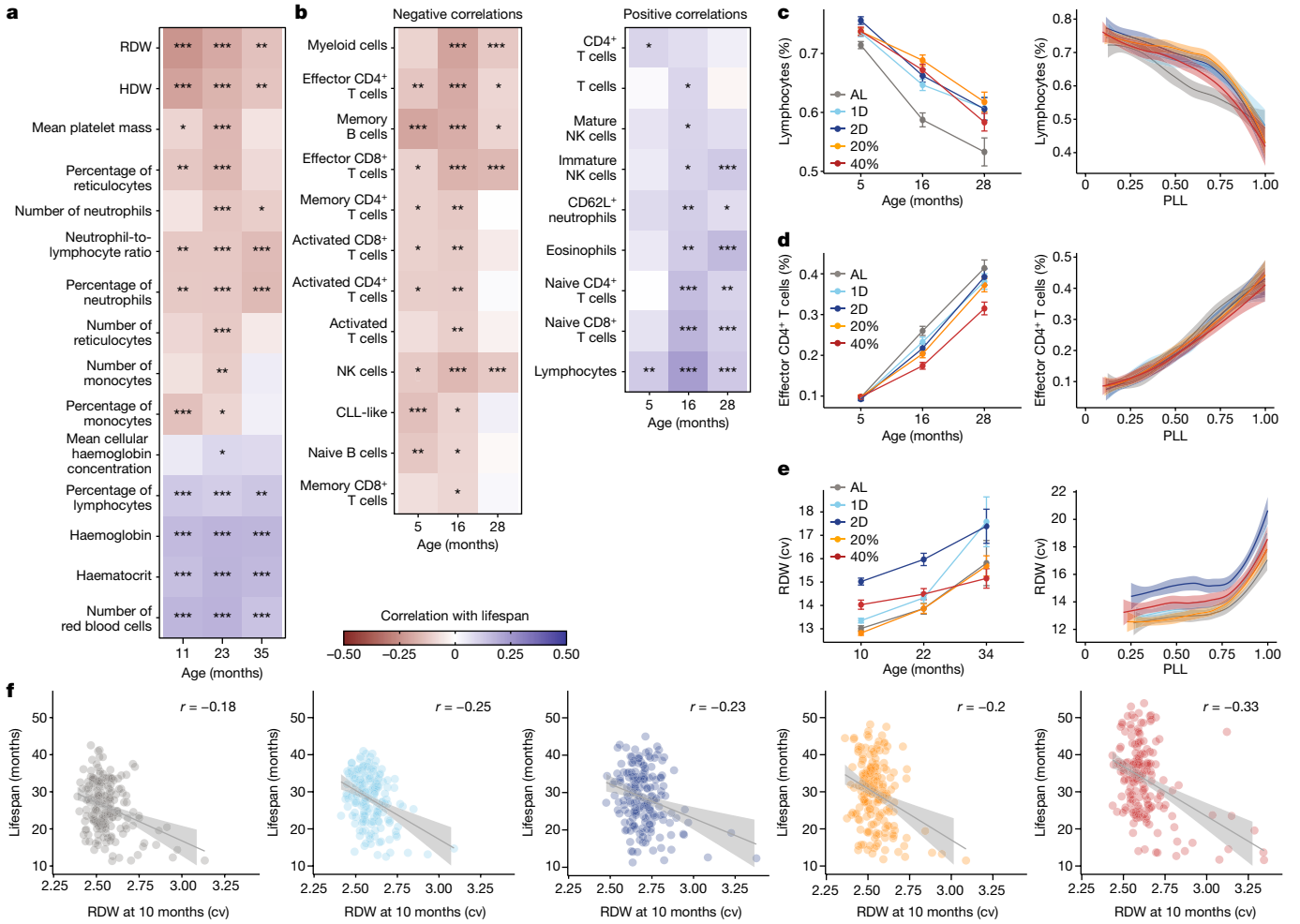

Fig. 4 | Immune and haematologic traits change with age, respond to diet and predict lifespan. a,**b**, Diet- and body-weight-adjusted correlation with lifespan for selected haematological traits from flow cytometry (**a**) and immune traits from complete blood counts (**b**) at the indicated ages. The asterisks indicate multiple-testing-adjusted significance, determined using linear regression of lifespan on traits; $^{*}P_{adj} < 0.01$, $^{**}P_{adj} < 0.001$, $^{***}P_{adj} < 0.0001$. **c**, Lymphocytes (the proportion of viable cells) by age (mean ± 2 s.e.m.; $n = 936$ (5 months), $n = 830$ (16 months), $n = 485$ (28 months) mice) and by PLL as loess smoothing with the 95% confidence bands (PLL: $P < 2.2 \times 10^{-16}$; diet: $P < 4.43 \times 10^{-8}$; diet × PLL: $P = 0.0670$). **d**, Effector CD4 T cells (proportion of all CD4 T cells) by age (mean ± 2 s.e.m.; sample sizes were as described in **c**) and by PLL as loess smoothing with the 95% confidence bands (PLL: $P < 2.2 \times 10^{-16}$; diet: $P = 0.268$; diet × PLL: $P = 0.300$). **e**, RDW (coefficient of variation (cv)) by age (mean ± 2 s.e.m.; $n = 892$ (10 months), $n = 665$ (22 months), $n = 208$ (34 months) mice) and by PLL as loess smoothing with the 95% confidence bands (PLL: $P < 2.2 \times 10^{-16}$; diet: $P < 2.2 \times 10^{-16}$; diet × PLL: $P = 4.77 \times 10^{-5}$). **f**, Lifespan by RDW at 10 months, with the regression line, 95% confidence bands and diet-specific correlations ($P_{adj} = 5.71 \times 10^{-11}$; diet × trait: $P = 0.395$, $r = -0.239$). Details of the statistical tests are provided in the 'Longitudinal trait analysis' (**c**–**e**) and 'Trait association with lifespan' (**f**) sections of the Methods. CLL, chronic lymphocytic leukaemia.

most of the erythroid traits exhibited significant positive associations (haemoglobin, haematocrit, red blood cell count) or negative associations (RDW, HDW) with lifespan (Fig. 4f and Extended Data Fig. 7k).

Mediation of DR effects on lifespan

Given the large number of traits that were both influenced by DR and associated with lifespan, we sought to estimate the fraction of overall effects of DR on lifespan that were explained by measured traits. We further sought to disentangle distinct effects of DR by identifying conditionally independent groups of traits as proxies for latent physiological processes with effects on lifespan. We first performed a multivariate network analysis across 194 traits that were assessed between 10 and 16 months of age, plus lifespan and diet, and fit a partial correlation network (sparse undirected Gaussian graphical model[47]). The network revealed groups of highly correlated traits clustered largely within phenotyping domains (Extended Data Fig. 8a and Supplementary Table 10) that we associated with important physiological variables such as energy expenditure. To identify conditionally independent effects, we selected a subset of 21 exemplar traits, one for each of the clusters in the full network. We then fit a reduced partial correlation network and performed a path analysis[48] to decompose the covariance between diet and lifespan (Extended Data Fig. 8b). In total, all paths through the measured traits explained 39% of the diet to lifespan covariance (Supplementary Table 11). The direct path (diet→lifespan) represents the remaining 61% of unexplained covariation. The next highest scoring path (diet→PhenoDelta→lifespan) explained 10.8% of the covariance and represents a negative effect of DR on lifespan. Another high scoring path (diet→ RDW→lifespan) also represents a negative effect of DR on lifespan that explained 0.7% of covariance. Several paths encompassing metabolic traits (energy expenditure, glucose, food intake) converge through LTM to explain 3.8% of the covariance. Other top scoring paths act through immune traits including lymphocytes, eosinophils and T cell classes and explained 7.5% of covariance. Although the selected traits are unlikely to be direct causal mediators of the DR effects on lifespan, they serve as surrogates for underlying mechanisms that mediate the effects of DR. Identification of these mechanisms could provide targets for interventions. However, the

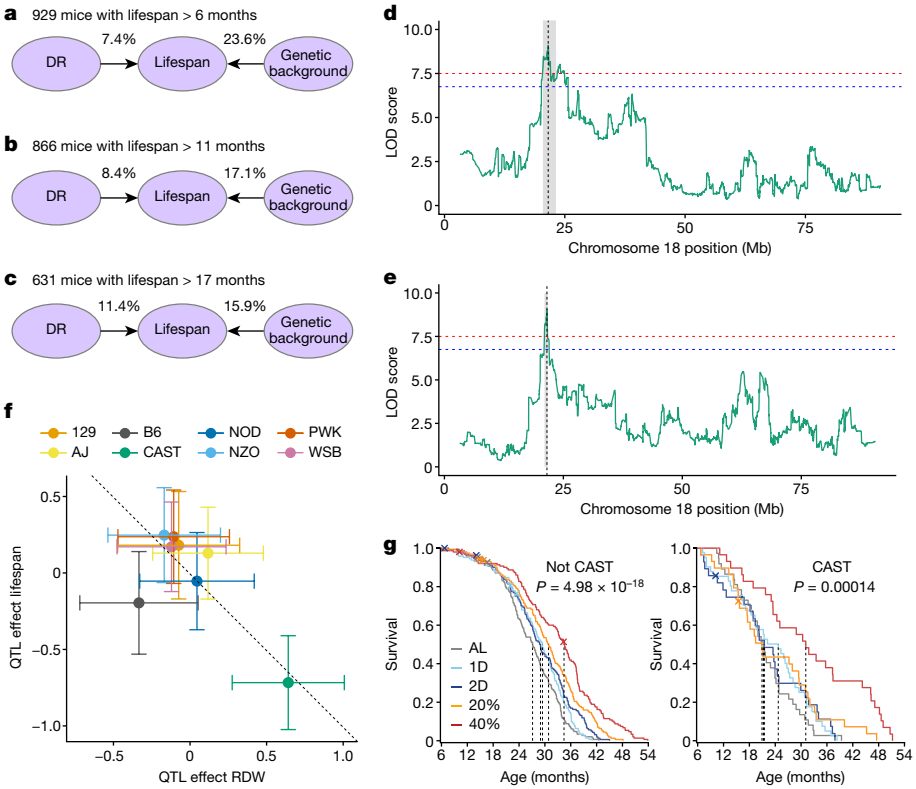

Fig. 5 | Genetic effects on lifespan in DO mice. a–**c**, The proportion of variance explained by genetics and DR to lifespan changes (>6 months (**a**), >11 months (**b**) and >17 months (**c**)) with age. **d**,**e**, Genetic mapping identifies genome-wide significant association with lifespan (**d**) and with RDW (**e**) on mouse chromosome 18. The *x* axis shows the genome position and the *y* axis shows the $\log_{10}$-transformed likelihood ratio (LOD score). **f**, Estimated additive genetic effects (centre) of each of the eight founder strain haplotypes (colour; A/J (AJ), C57BL/6J (B6), 129S1/SvlmJ (129), NOD/ShiLtJ (NOD), NZO/HILtJ (NZO), CAST/EiJ (CAST), PWK/PhJ (PWK) and WSB/EiJ(WSB)) at the chromosome 18 QTL for RDW (*x* axis) and lifespan (*y* axis) (regression coefficient ± 1 s.e.m.; $n = 892$ mice). The reference line (dotted) has a slope of −1 and an intercept of 0. **g**, Kaplan–Meier survival curves by diet group (colour) are shown for mice stratified by the presence of a CAST allele at the QTL. The dashed lines indicate the median survival age per group. Significance was calculated using log-rank test comparison across diets within genotype strata. $n = 765$ (not CAST) and $n = 164$ (CAST).

multiplicity of independent paths and the mix of paths with consistent and inconsistent effects supports a pleiotropic model of DR effects on lifespan. Notably, the effects of DR on several traits, including those that are most strongly associated with lifespan, such as body weight loss during phenotyping and RDW, show effects that were opposite to the direct effects of DR on lifespan.

Genetic determinants of lifespan

We obtained whole-genome genotyping data for 929 (out of 937) mice and looked at the combined effects of diet and genetics on lifespan. For mice that lived to at least 6 months of age, genetic background explained 23.6% of variation in lifespan ($h^2 = 0.236$, 95% bootstrap confidence interval 0.106–0.360), while diet explained only 7.4% of variation. As mice aged, heritability declined to 17.1% for mice surviving past 12 months and to 15.9% for mice surviving past 18 months. In parallel, the contribution of diet to lifespan increased with age to 8.4% at 12 months and to 11.4% at 18 months. Similar trends of decreasing genetic effect and increasing effects of DR were previously reported for body weight[49] (Fig. 5a–c).

We performed genetic mapping analysis of the physiological traits and identified 300 significant quantitative trait loci (QTL; genome-wide adjusted $P < 0.05$; Extended Data Fig. 9 and Supplementary Table 12). A significant QTL for lifespan mapped to chromosome 18 at 21.55 Mb (95% support interval = 20.44–24.92; Fig. 5d and Extended Data Fig. 10a). The QTL explained 4.34% of the diet-adjusted variance in lifespan, corresponding to 23.4% of the total genetic effect. Even though more than 75% of the genetic contribution to lifespan remained unexplained, we did not detect any additional significant QTL for lifespan.

Among the physiological traits, RDW at 10 months was the only trait with a QTL that co-located with the lifespan QTL (RDW QTL at 21.55 Mb, 95% support interval = 21.06–21.61; Fig. 5e and Extended Data Fig. 10b). We estimated the additive genetic contribution of founder haplotypes (the DO mice are descended from eight inbred founder strains) at these QTL and found that both were driven by the CAST/EiJ (CAST) founder haplotype (Fig. 5f). The presence of the CAST haplotype at this locus was associated with reduced lifespan and with higher RDW. Among the 164 mice (out of 929) with at least one copy of the CAST haplotype at this locus, lifespan was reduced by an average of 3.7 months (12.5%, $P = 6.66 \times 10^{-7}$). Kaplan–Meier analysis of lifespan, stratified by the presence or absence of the CAST allele at the QTL, confirmed that diet had a significant effect on lifespan in both genotype groups (Fig. 5g). Furthermore, mice carrying a CAST allele at the QTL showed reduced lifespan, with the possible exception of the 40% CR group, for which the within-diet test of genotype effect was not significant (Extended Data Fig. 10c and Supplementary Table 13).

Variant association mapping of lifespan and RDW (Extended Data Fig. 10d,e) narrowed the QTL to a region that encompasses around 20 positional candidate genes, including *Garem1*, *Klhl14*, *Asxl3*, *Mep1b*, *Rnf138* and *Rnf125*, and a cluster of desmocollin and desmoglein family members (*Dsc* and *Dsg*). The latter have a plausible functional role in maintaining structure and size of red blood cells. Loss of function of *Garem1*, the gene closest to the strongest variant association, is

associated with spleen size and morphology in mice[50], suggesting a plausible link to RDW through recycling of red blood cells. Among the other candidate genes, we identified one (*Dsc2*) with an eQTL in mouse liver that is associated with CAST alleles (https://qtlviewer.jax.org/#datasets). There are 34 missense variants with private CAST alleles across 11 genes in the QTL region, including *Garem1*[51]. RDW has been associated with lifespan in human studies[52]. Although several hundred human GWAS associations with RDW have been reported[53,54], none appear to be homologous to the mouse chromosome 18 QTL or colocalize with GWAS associations for human lifespan. Definitive identification of a causal gene candidate could shed further light on the mechanism linking RDW and lifespan.

Discussion

Here we report the effects of graded levels of CR and IF on the health and lifespan of almost 1,000 female DO mice in which we longitudinally profiled hundreds of physiological traits. Collectively, our study highlighted physiological resilience, in particular the maintenance of body weight, body composition and key immune cell populations, as major biomarkers for longevity and suggested that the pro-longevity effects of DR may be uncoupled from its effects on metabolic traits. Despite the powerful effects of DR in this study, genetic background proved to be the more important factor in determining lifespan.

Our results have several important implications (Supplementary Discussion). First, they suggest a divergence of the health and longevity effects of DR. Several well-described impacts of DR on metabolic health, such as improved fasting blood glucose, energy expenditure and oscillations in respiratory quotient, did not predict lifespan within diet groups. This means that, although DR-induced changes in metabolic traits can be beneficial for health, they may not necessarily translate into a substantial extension of lifespan. This insight has important implications for the choice of biomarkers in human dietary intervention studies, which frequently focus on metabolic health[55].

Second, our findings more generally imply that the effects of DR on health and lifespan may be partially non-overlapping, and certain lifespan-extending properties of DR may in fact be detrimental to other aspects of physiological health. For example, although mice on 40% CR are healthy by most measures, we saw indications of adverse effects including life-long loss of lean mass, lower body temperature, food-seeking behaviour (an indication of hunger) and changes in immune repertoire that could potentially confer susceptibility to infection. These effects in mice may raise concerns regarding the potential risks of extreme DR for humans.

Finally, whether IF and CR would extend lifespan in humans awaits definitive investigation[56]. Owing to differences in metabolic rates, the human equivalent of these DR interventions is unclear. Although further work is needed to dissect the complex physiological effects of DR, our findings suggest that human responses to DR will be highly individualized based on genetic context, that moderate reduction of caloric intake and regular daily feeding and fasting cycles are key contributing factors[7,8], and that specific blood biomarkers can predict an individual's ability to benefit from certain physiological effects of DR, while withstanding others, to maximize its health benefits and longevity effects.

Online content

Any methods, additional references, Nature Portfolio reporting summaries, source data, extended data, supplementary information, acknowledgements, peer review information; details of author contributions and competing interests; and statements of data and code availability are available at https://doi.org/10.1038/s41586-024-08026-3.

1. Fontana, L., Partridge, L. & Longo, V. D. Extending healthy life span—from yeast to humans. *Science* **328**, 321–326 (2010).
2. Di Francesco, A., Di Germanio, C., Bernier, M. & de Cabo, R. A time to fast. *Science* **362**, 770–775 (2018).
3. Longo, V. D. & Panda, S. Fasting, circadian rhythms, and time-restricted feeding in healthy lifespan. *Cell Metab.* **23**, 1048–1059 (2016).
4. de Cabo, R. & Mattson, M. P. Effects of intermittent fasting on health, aging, and disease. *N. Engl. J. Med.* **381**, 2541–2551 (2019).
5. Duregon, E. et al. Prolonged fasting times reap greater geroprotective effects when combined with caloric restriction in adult female mice. *Cell Metab.* **35**, 1179–1194 (2023).
6. Mitchell, S. J. et al. Daily fasting improves health and survival in male mice independent of diet composition and calories. *Cell Metab.* **29**, 221–228 (2019).
7. Pak, H. H. et al. Fasting drives the metabolic, molecular and geroprotective effects of a calorie-restricted diet in mice. *Nat. Metab.* **3**, 1327–1341 (2021).
8. Acosta-Rodriguez, V. et al. Circadian alignment of early onset caloric restriction promotes longevity in male C57BL/6J mice. *Science* **376**, 1192–1202 (2022).
9. Green, C. L., Lamming, D. W. & Fontana, L. Molecular mechanisms of dietary restriction promoting health and longevity. *Nat. Rev. Mol. Cell Biol.* **23**, 56–73 (2022).
10. Forster, M. J., Morris, P. & Sohal, R. S. Genotype and age influence the effect of caloric intake on mortality in mice. *FASEB J.* **17**, 690–692 (2003).
11. Mitchell, S. J. et al. Effects of sex, strain, and energy intake on hallmarks of aging in mice. *Cell Metab.* **23**, 1093–1112 (2016).
12. Vaughan, K. L. et al. Caloric restriction study design limitations in rodent and nonhuman primate studies. *J. Gerontol. A* **73**, 48–53 (2017).
13. Hofer, S. J. & Madeo, F. Sex- and timing-specific effects of fasting and caloric restriction. *Cell Metab.* **35**, 1091–1093 (2023).
14. Suchacki, K. J. et al. The effects of caloric restriction on adipose tissue and metabolic health are sex- and age-dependent. *eLife* **12**, e88080 (2023).
15. Liao, C. Y., Rikke, B. A., Johnson, T. E., Diaz, V. & Nelson, J. F. Genetic variation in the murine lifespan response to dietary restriction: from life extension to life shortening. *Aging Cell* **9**, 92–95 (2010).
16. Hahn, O. et al. A nutritional memory effect counteracts benefits of dietary restriction in old mice. *Nat. Metab.* **1**, 1059–1073 (2019).
17. Colman, R. J. et al. Caloric restriction reduces age-related and all-cause mortality in rhesus monkeys. *Nat. Commun.* **5**, 3557 (2014).
18. Catenacci, V. A. et al. A randomized pilot study comparing zero-calorie alternate-day fasting to daily caloric restriction in adults with obesity. *Obesity* **24**, 1874–1883 (2016).
19. Cioffi, I. et al. Intermittent versus continuous energy restriction on weight loss and cardiometabolic outcomes: a systematic review and meta-analysis of randomized controlled trials. *J. Transl. Med.* **16**, 371 (2018).
20. Lowe, D. A. et al. Effects of time-restricted eating on weight loss and other metabolic parameters in women and men with overweight and obesity: the TREAT randomized clinical trial. *JAMA Intern. Med.* **180**, 1491–1499 (2020).
21. Harvie, M. & Howell, A. Potential benefits and harms of intermittent energy restriction and intermittent fasting amongst obese, overweight and normal weight subjects—a narrative review of human and animal evidence. *Behav. Sci.* **7**, 4 (2017).
22. Heilbronn, L. K., Smith, S. R., Martin, C. K., Anton, S. D. & Ravussin, E. Alternate-day fasting in nonobese subjects: effects on body weight, body composition, and energy metabolism. *Am. J. Clin. Nutr.* **81**, 69–73 (2005).
23. Horne, B. D., Grajower, M. M. & Anderson, J. L. Limited evidence for the health effects and safety of intermittent fasting among patients with type 2 diabetes. *JAMA* **324**, 341–342 (2020).
24. Hofer, S. J., Carmona-Gutierrez, D., Mueller, M. I. & Madeo, F. The ups and downs of caloric restriction and fasting: from molecular effects to clinical application. *EMBO Mol. Med.* **14**, e14418 (2022).
25. Svenson, K. L. et al. High-resolution genetic mapping using the mouse diversity outbred population. *Genetics* **190**, 437–447 (2012).
26. Bou Sleiman, M. et al. Sex- and age-dependent genetics of longevity in a heterogeneous mouse population. *Science* **377**, eabo3191 (2022).
27. Harrill, A. H. et al. *NTP Research Report on Baseline Characteristics of Diversity Outbred (J:DO) Mice Relevant to Toxicology Studies* NTP Research Report 6 (2018).
28. Hambly, C. & Speakman, J. R. Mice that gorged during dietary restriction increased foraging related behaviors and differed in their macronutrient preference when released from restriction. *PeerJ* **3**, e1091 (2015).
29. Acosta-Rodriguez, V. A., de Groot, M. H. M., Rijo-Ferreira, F., Green, C. B. & Takahashi, J. S. Mice under caloric restriction self-impose a temporal restriction of food intake as revealed by an automated feeder system. *Cell Metab.* **26**, 267–277 (2017).
30. Wang, C., Li, Q., Redden, D. T., Weindruch, R. & Allison, D. B. Statistical methods for testing effects on maximum lifespan. *Mech. Ageing Dev.* **125**, 629–632 (2004).
31. Hughes, B. G. & Hekimi, S. Different mechanisms of longevity in long-lived mouse and *Caenorhabditis elegans* mutants revealed by statistical analysis of mortality rates. *Genetics* **204**, 905–920 (2016).
32. Miller, R. A., Harper, J. M., Galecki, A. & Burke, D. T. Big mice die young: early life body weight predicts longevity in genetically heterogeneous mice. *Aging Cell* **1**, 22–29 (2002).
33. Roy, S. et al. Gene-by-environment modulation of lifespan and weight gain in the murine BXD family. *Nat. Metab.* **3**, 1217–1227 (2021).
34. Kraus, C., Pavard, S. & Promislow, D. E. The size-lifespan trade-off decomposed: why large dogs die young. *Am. Nat.* **181**, 492–505 (2013).
35. Goodrick, C. L., Ingram, D. K., Reynolds, M. A., Freeman, J. R. & Cider, N. Effects of intermittent feeding upon body weight and lifespan in inbred mice: interaction of genotype and age. *Mech. Ageing Dev.* **55**, 69–87 (1990).
36. Martin, B., Ji, S., Maudsley, S. & Mattson, M. P. "Control" laboratory rodents are metabolically morbid: why it matters. *Proc. Natl Acad. Sci. USA* **107**, 6127–6133 (2010).
37. Liao, C. Y. et al. Fat maintenance is a predictor of the murine lifespan response to dietary restriction. *Aging Cell* **10**, 629–639 (2011).

38. Whitehead, J. C. et al. A clinical frailty index in aging mice: comparisons with frailty index data in humans. *J. Gerontol. A* **69**, 621–632 (2014).
39. Speakman, J. R. & Mitchell, S. E. Caloric restriction. *Mol. Aspects Med.* **32**, 159–221 (2011).
40. Redman, L. M. et al. Metabolic slowing and reduced oxidative damage with sustained caloric restriction support the rate of living and oxidative damage theories of aging. *Cell Metab.* **27**, 805–815 (2018).
41. Nikolich-Zugich, J. Aging of the T cell compartment in mice and humans: from no naive expectations to foggy memories. *J. Immunol.* **193**, 2622–2629 (2014).
42. Alpert, A. et al. A clinically meaningful metric of immune age derived from high-dimensional longitudinal monitoring. *Nat. Med.* **25**, 487–495 (2019).
43. Lin, Y. et al. Changes in blood lymphocyte numbers with age in vivo and their association with the levels of cytokines/cytokine receptors. *Immun. Ageing* **13**, 24 (2016).
44. Whiting, C. C. et al. Large-scale and comprehensive immune profiling and functional analysis of normal human aging. *PLoS ONE* **10**, e0133627 (2015).
45. Guralnik, J. M., Eisenstaedt, R. S., Ferrucci, L., Klein, H. G. & Woodman, R. C. Prevalence of anemia in persons 65 years and older in the United States: evidence for a high rate of unexplained anemia. *Blood* **104**, 2263–2268 (2004).
46. Lippi, G. & Plebani, M. Red blood cell distribution width (RDW) and human pathology. One size fits all. *Clin. Chem. Lab. Med.* **52**, 1247–1249 (2014).
47. Chen, Z. et al. Automated, high-dimensional evaluation of physiological aging and resilience in outbred mice. *eLife* **11**, e72664 (2022).
48. Jones, B. & West, M. Covariance decomposition in undirected Gaussian graphical models. *Biometrika* **92**, 779–786 (2005).
49. Wright, K. M. et al. Age and diet shape the genetic architecture of body weight in diversity outbred mice. *eLife* **11**, e64329 (2022).
50. Baldarelli, R. M. et al. Mouse Genome Informatics: an integrated knowledgebase system for the laboratory mouse. *Genetics* **227**, iyae031 (2024).
51. Ball, R. L. et al. GenomeMUSter mouse genetic variation service enables multitrait, multipopulation data integration and analysis. *Genome Res.* **34**, 145–159 (2024).
52. Patel, K. V., Ferrucci, L., Ershler, W. B., Longo, D. L. & Guralnik, J. M. Red cell distribution width and the risk of death in middle-aged and older adults. *Arch. Intern. Med.* **16**, 515–523 (2009).
53. Pan, J. et al. Red cell distribution width and its polygenic score in relation to mortality and cardiometabolic outcomes. *Front. Cardiovasc. Med.* **10**, 1294218 (2023).
54. Pilling, L. C. et al. Red blood cell distribution width: genetic evidence for aging pathways in 116,666 volunteers. *PLoS ONE* **12**, e0185083 (2017).
55. Palliyaguru, D. L. et al. Fasting blood glucose as a predictor of mortality: lost in translation. *Cell Metab.* **33**, 2189–2200.e3 (2021).
56. Kebbe, M., Sparks, J. R., Flanagan, E. W. & Redman, L. M. Beyond weight loss: current perspectives on the impact of calorie restriction on healthspan and lifespan. *Expert Rev. Endocrinol. Metab.* **16**, 95–108 (2021).

Methods

Mice

We enrolled 960 female DO mice in 12 waves, corresponding to birth cohorts from generations 22 to 24 and 26 to 28 with 80 first-parity and 80 second-parity animals from each generation born around 3 weeks apart. No more than one mouse per litter was enrolled in the study. The first cohort entered the study in March 2016 and the study was fully populated in November 2017. This schedule was designed to make efficient use of our phenotyping capacity and minimize the potential for seasonal confounding. The sample size was determined to detect a 10% change in mean lifespan between intervention groups with allowance for some loss of animals due to non-age-related events. We used female mice due to concerns about male aggression. Mice were assigned to housing groups of eight animals in large-format wean boxes with positive pressure ventilation and incoming air temperature of 24.4 to 25.6 °C. Environmental enrichments were provided including nestlets, biotubes and gnawing blocks. Mice were randomized by housing group to one of five dietary interventions. Blinding was not possible due to the different feeding requirements in each intervention group. Of the 960 mice that were entered into the study, 937 mice were alive when interventions were initiated at 6 months of age and only these mice are included in our analysis. All of the procedures used in the study were reviewed and approved under Jackson Lab IACUC protocol 06005.

DR

DR was implemented by controlling the timing and amount of food provided to mice. Feeding schedules for DR were started at 6 months of age. All mice were fed a standard mouse chow diet (5K0G, LabDiet). The AL feeding group was provided with unlimited access to food and water. The IF mice were provided unlimited access to food and water. On Wednesday of each week at 15:00, IF mice were placed into clean cages and food was withheld for the next 24 or 48 h for the 1D and 2D groups, respectively. CR mice were provided with unlimited access to water and measured amounts of food daily at around 15:00, 2.75 g per mouse per day for 20% CR and 2.06 g per mouse per day for 40% CR. These amounts were based on AL consumption of 3.43 g per mouse per day that we estimated based on historical feeding data from DO mice. For the 40% CR protocol, a gradual reduction in food intake was implemented: the mice were first subjected to 20% CR for 2 weeks, then to 30% CR for an additional 2 weeks, before transitioning to the full 40% CR. In the 2D IF protocol, mice were initially acclimatized to the 1D IF regimen for 2 weeks. Mice were co-housed with up to eight mice per pen. Co-housing is standard practice for CR studies[39]; competition for food was minimized by placing food directly into the bottom of the cage, allowing individual mice to 'grab' a pellet and isolate while they eat. CR mice were provided with a 3 day ration of food on Friday afternoon, which resulted in weekly periods of feasting followed by a period of food deprivation of approximately 1 day for the 20% CR mice and 2 days for the 40% CR mice, comparable to the IF fasting periods. The 15:00 feeding time closely approximates the circadian alignment of feeding, starting just before the beginning of the dark cycle, which is the normal active and feeding time of day for mice. This timing has been shown to maximize lifespan extension in mice subjected to 30% CR[8]. The feast–famine cycle induced by the Friday triple feeding has been used in other studies of CR[57–59] but direct assessment of the health impacts is lacking.

Food intake (160 mouse independent cohort)

To obtain an accurate estimate of food intake and changes in body weight in response to weekly fasting cycles, we set up an independent cohort of 160 female DO mice. Mice were placed on the same DR protocols as in the main study. Food was weighed daily for a period of 1 week when mice were 30, 36 and 43 weeks of age. Food intake data were normalized to units of g per mouse per day and presented as daily and weekly averages across timepoints by diet. Body composition was determined at 43 and 45 weeks of age using non-imaging nuclear magnetic resonance (NMR) using the Echo MRI instrument, a NMR device with a 5-gauss magnet that is adapted to small-animal studies. NMR data were used to detect changes in body weight and composition before and after fasting. Values of body weight, lean mass, fat mass and adiposity (100% × fat mass/total mass) pre-fasting were co-plotted with the difference between before and after fasting (Friday to Monday for AL and CR; Tuesday to Thursday for 1D IF; Tuesday to Friday for 2D IF).

Phenotyping

We performed three cycles of health assessments of mice at early, middle and late life. These assessments included a 7-day metabolic cage run at around 16, 62 and 114 weeks of age; blood collection for flow cytometry analysis at 24, 71 and 122 weeks; rotarod, body composition, echocardiogram, acoustic startle, bladder function, free wheel running and a blood collection for CBC analysis at around 44, 96 and 144 weeks of age. Furthermore, body weights were recorded weekly and manual frailty and grip strength assessments were carried out at 6 month intervals. All assays were conducted at the Jackson Laboratory according to standard operating procedures.

Body weight. Mice were weighed weekly throughout their lives, resulting in over 100,000 values longitudinally collected for the 937 mice. Body weights were analysed after local polynomial regression fitting within mouse (that is, loess smoothing).

Frailty, grip strength and body temperature. We applied a modified version of the clinically relevant FI[38], which was calculated as the average of 31 traits that are indicators of age-associated deficits and health deterioration. Each trait was scored on a scale of 0, 0.5 or 1, where 0 indicated the absence of the deficit; 0.5 indicated mild deficit; and 1 indicated severe deficit. Measurements were taken at the baseline (5 months) and were repeated approximately every 6 months. Simple averaging yielded a raw FI score of between 0 and 1 for each mouse. Frailty scores were adjusted by estimating batch, coat colour and experimenter effects as random factors that were subtracted from raw frailty score values before statistical analysis.

Body composition. We performed dual X-ray absorptiometry analysis using the LUNAR PIXImus II densitometer to collect bone density and body composition (including fat and non-fat lean tissue). Mice were anaesthetized and individually placed onto a disposable plastic tray that was then placed onto the exposure platform of the PIXImus. The process to acquire a single scan lasts approximately 4 min. Measurements were taken at around 44, 96 and 144 weeks of age.

Immune cell profiling using flow cytometry. Peripheral blood samples were analysed by flow cytometry to determine the frequency of major circulating immune cell subsets. Analysis was performed before the start of dietary interventions at 5 months, then at 16 and 24 months of age. These timepoints corresponded to 11 and 19 months of dietary intervention. Red blood cells in PBL samples were lysed and the samples were washed in FACS buffer (Mitenyi, 130-091-222). Cells were resuspended in 25 µl FACS buffer with 0.5% BSA (Miltenyi, 130-091-222 with 130-091-376). Antibodies including Fc block (2.42, Leinco Technologies) were added and incubated for 30 min at 4 °C. Labelled cells were washed and DAPI was added before analysis on the LSRII (BD Bioscience) system. The antibody cocktail contained CD11c FITC, N418 (35-0114-U100, Tonbo Biosciences, 1:100); NKG2D (CD314) PE, CX5 (558403, BD Biosciences, 1:80); CD3e PE-CF594, 145-2C11 (562286, BD Biosciences, 1:40); CD19 BB700, 1D3 (566411, BD Biosciences, 1:40); CD62L PE-Cy7, MEL-14, (60-0621-U100, Tonbo Biosciences, 1:100); CD25 APC, PC61 (102012, BioLegend, 1:80); CD44 APC-Cy7, IM7 (25-0441-U100, Tonbo Biosciences, 1:40); Ly6G BV421, 1A8, (562737, BD

Biosciences, 1:80); CD4 BV570, RM4-5 (100542, BioLegend, 1:40); CD11b BV650, M1/70 (563402, BD Biosciences, 1:160); CD45R/B220 BUV496 (RA3-6B2, 564662, BD Biosciences, 1:20); Fc Block, 2.4G2 (C247, Leinco Technologies, 1:100).

Owing to the outbred nature of these mice, flow cytometry markers were limited, and T cell subsets were generally assigned as naive and non-naive by the presence of CD62L and CD44 (immune cell subtype designations are shown in Supplementary Table 7). NKG2D-positive cells were enumerated and may represent memory T cells that accumulate after immune responses[60]. Owing to limitations in flow cytometry markers that identify NK cells and their subsets in the mouse strains contributing to the outbred DO mouse line, NK cells were defined as non-T non-B lymphocytes expressing NKG2D. Within this population, CD11c and CD11b were used to generally define maturation subsets. CD11b expression marks more mature NK cells and CD11c is reduced on the least-mature NK subset[61].

Glucose. At the flow cytometry blood collections at 16, 62 and 114 weeks, mice were fasted for 4 h and glucose was measured using the OneTouch Ultra2 glucose meter from LifeScan along with OneTouch Ultra test strips. At each of the CBC blood collections at 24, 71 and 122 weeks, non-fasted glucose was measured using the glucose meter.

Echocardiogram. Ultrasonography was performed using the VisualSonics (VSI) Vevo 770/2100 high-frequency ultrasound system with 30 and 40 MHz probes. Echocardiography uses pulsed Doppler sonography, applied through the ultrasound probe, to measure blood flow rates and volumes.

Metabolic monitoring cages. Mice were individually housed for 7 days in a metabolic cage (Promethion Model from Sable Systems International) and the activity, feeding and respiration were tracked. Feeding protocols for dietary intervention were maintained. Metabolic cage data were used to assess metabolism, energy expenditure and activity of mice in Y1, Y2 and Y3. Animal-level data were cleaned to remove outliers and instrument failure and summarized as cumulative (food, wheel distance) or median across 5 min intervals (respiratory quotient, energy expenditure). The mean and s.d. were computed at 4 h and 1 h intervals and were plotted as mean ± 2 s.e.m. across timepoint intervals. Animal-level summaries were computed as the average across 7 days of the daily (24 h), light phase (12 h) or dark phase (12 h) median values. Moreover, we computed 'change' traits (for example, delta respiratory quotient and delta energy expenditure) as the difference between the 5th to 95th percentiles of all 1 h summaries across the entire 7 day run.

CBC analysis. Blood samples were run on the Siemens ADVIA 2120 haematology analyzer with mouse-specific software as described previously[62].

Acoustic startle. Startle response was measured in rodents using automated startle chambers, in which a mouse was placed in a clear, acrylic tube attached to a highly sensitive platform that is calibrated to track their startle reflex while being exposed to a series of stimuli at varying decibels and times. Mice were initially exposed to white noise from an overhead speaker, which transitions to a series of randomized, computer-generated stimuli ranging in volume from 70 to 120 decibels at 40 ms in duration and an interval of 9–22 s. The test runs for approximately 30 min.

Rotarod. We used the Ugo–Basile rotarod, which has five lanes evenly spaced along a motorized horizontal rotating rod, allowing for up to five mice to be tested simultaneously. Below each lane is a platform equipped with a trip plate that records the latency for each mouse to fall. At the beginning of the session, mice were placed onto the rod, which began rotating at 4 rpm, slowly increasing to a maximum of 40 rpm, over 300 s. Mice were given three consecutive trials. We reported the mean latency (time to fall) and the slope of latencies across trials, as well as the number of trials with no falls and number of trials with immediate falls. In case a mouse did not cooperate with the test, trials were recorded as missing.

Voiding assay. Cages were prepared by cutting a piece of cosmos blotting paper, 360 gsm, to standard duplex cage dimensions. Shavings were removed from a clean cage, and the paper was taped to the bottom of the cage. Food was provided during this test; however, water was removed to prevent possible leaking onto the blotting paper. Mice were individually housed in a prepared cage for 4 h. At the end of the trial, the mice were returned to their original housing units, and papers were removed and dried for 2–4 h, before being individually bagged. Papers were shipped to Beth Israel Deaconess Medical Center, where they were scanned with ultraviolet light to image and quantify the void spots.

Home cage wheel running. Free-wheel-running data were collected at around 44, 96 and 144 weeks of age. Mice were individually housed for a minimum of 36 h in a special cage suited to house the Med Associate low profile running wheel with a wireless transmitter. The food hopper was removed to allow for seamless movement of the wheel, and food was placed onto the cage floor. The 15.5-cm-diameter plastic wheel sits at an angle on an electronic base, which tracks the revolutions. The battery-powered base allows for continuous monitoring of data, which is then wirelessly transmitted, in 30 s intervals, to a local computer.

Lifespan. Research staff regularly evaluated mice for prespecified clinical symptomology: palpable hypothermia, responsiveness to stimuli, ability to eat or drink, dermatitis, tumours, abdominal distention, mobility, eye conditions (such as corneal ulcers), malocclusion, trauma and wounds of aggression. If mice met the criteria for observation in any of these categories, veterinary staff were contacted. If the clinical team determined a mouse to be palpably hypothermic and unresponsive, unable to eat or drink, and/or met protocol criteria for severe dermatitis, tumours and/or fight wounds, pre-emptive euthanasia was performed to prevent suffering; otherwise, the veterinary staff provided treatment. Both mice euthanized or found dead were represented as deaths in the survival curves. Mice euthanized due to injuries unrelated to imminent death were treated as censored (we recorded a total of 13 censoring events).

Data preparation and analysis

Cloud-based research management software (Climb by Rockstep) was used to track animals, schedule testing and provide a stable repository for primary data collection. Data were regularly reviewed by a statistical analyst during the study for anomalies. Initial data quality control included identifying and resolving equipment miscalibration, mislabelled animals and technically impossible values. If we could not manually correct these using laboratory records, they were removed. Quantitative assays including body weight and temperature were explored for outliers. Quantitative traits other than body weights were corrected for batch effects. To quantify batch effects, we fit a fully random-effects linear mixed model conditioning on diet, body weight at test and age. We adjusted trait values by subtracting the batch model coefficients. Lifespan data were recorded in days but are presented in months (30.4 days per month) for ease of interpretation. Statistical significance for extremely small P values is reported as $P < 2.2 \times 10^{-16}$ in the main text; non-truncated P values are provided in the Supplementary Information. All analyses were performed using R v.4.2.2 and RStudio v.2022.12.0+353. Data analysis scripts are available (Data availability).

Survival analysis. We performed survival analysis to compare lifespan outcomes for the five study groups. We plotted Kaplan–Meier survival curves and tested the equality of survival distributions across diet

groups using log rank tests using an overall test (4 d.f.) and all pairwise comparisons between diets. *P* values are reported with no multiple testing adjustment, and we considered a comparison to be significant if $P < 0.01$. We estimated the median and maximum lifespan (90% survival) by diet group with 95% confidence intervals and percentage change relative to the AL group[30]. Mortality doubling times were estimated from a Gompertz log-linear hazard model with 95% CI and percentage change relative to the AL group (flexsurv R package v.2.2.2).

Longitudinal trait analysis. For traits collected annually or biannually, we were able to explore hypothesized direct and indirect relationships with diet, body weight and age. We used generalized additive mixed models (GAMMs) with a gaussian/identity link to analyse these effects by fitting a series of nonlinear relationships between trait response and covariates. GAMMs for a combination of fixed and random effects (formulae below) on trait response pre-adjusted for batch were fit using the gam() function of the mgcv package in R, with the Newton optimizer and default control parameters. Age was rescaled to proportion of life lived (PLL = age at test/lifespan). The PLL scale removes artifacts due to survivorship bias across groups with different lifespans. All continuous variables except for PLL were rank normal scores transformed (RZ) prior to model fitting.

(1) RZ(*T*) ~ D + s(BW) + s(PLL) + (1|ID)
(2) RZ(*T*) ~ D + s(PLL) + (1|ID)
(3) RZ(*T*) ~ D + s(BW) + (1|ID)
(4) RZ(*T*) ~ s(BW) + s(PLL) + (1|ID)
(5) RZ(*T*) ~ D + s(BW) + s(PLL|diet) + (1|ID)

where *T* is trait, *D* is dietary assignment, BW is body weight at the date closest to *T*'s collection date, PLL is the proportion of life lived as of *T* collection date and s() is the smoothing parameter. Each mouse had multiple datapoints across the *T* collection date. This clustering was accounted for with a random intercept for ID, specified as (1|ID) above. We performed hypothesis tests related to the GAMM fits to explore trait sensitivity to body weight (model 1 (M1) versus M2), PLL, (M1 versus M3), diet (M1 versus M4) and diet-by-trait interaction (M1 versus M5). Using the models specified above and a conservative false-discovery rate (FDR < 0.01, one-step Benjamini–Hochberg method), we therefore identified traits that responded additively to body weight, traits that responded additively to diet, traits that responded additively to PLL (scaled age) and traits that responded interactively to diet and PLL. Traits were categorized as health, metabolism, haematology or immune. For each trait category, bar plots were generated to show the number of traits with significant (FDR < 0.01) associations with body weight, diet, PLL and diet × PLL interactions. We repeated the same analysis with age (age in months) in place of PLL. We applied FDR adjustment to each test across traits and timepoints (Benjamini–Hochberg FDR method).

The complete results of the longitudinal trait analysis are provided in Supplementary Table 6.

Trait associations with lifespan. To identify traits that are associated with lifespan, we performed regression analysis on lifespan with traits at each timepoint after adjusting for effects of diet and body weight. We fit linear models:

(1) Lifespan ~ diet + BW6 + BW_{test},
(2) Lifespan ~ diet + BW6 + BW_{test} + trait
(3) Lifespan ~ diet + BW6 + BW_{test} + trait + diet:trait

where BW6 is the last preintervention body weight, and BW_{test} is the body weight at time of testing. For body composition and change-in-body weight traits, we did not include the body weight terms. All continuous variables were rank normal scores (RZ) transformed before model fitting. We performed likelihood ratio tests for the diet and body weight adjusted association (M2 versus M1) and for the diet × trait interaction (M3 versus M2). We applied a FDR adjustment to each test across traits and timepoints (one-step Benjamini–Hochberg method). Traits were categorized and significant (FDR < 0.01) results were tabulated as above.

We estimated the overall strength of association between trait and lifespan as the regression coefficient of the trait term in M2. As the traits are standardized, the regression coefficients are equivalent to diet- and body-weight-adjusted partial correlations (designated as *r*) and can be compared across traits. Moreover, we stratified the data to estimate diet-specific body-weight-adjusted partial correlations that are shown in the scatter plot panels (Fig. 2f).

The complete results of lifespan association analysis are provided in Supplementary Table 7.

Network modelling. We performed a multivariate network analysis to decompose the effects of DR on lifespan across measured traits. An empirical covariance matrix was estimated using the nonparanormal SKEPTIC estimator derived from the pairwise Kendall–Tau correlation using pairwise-complete data. The estimated covariance matrix was projected to the nearest positive definite matrix by truncating eigenvectors with negative eigenvalues. A sparse low-rank Gaussian graphical model was fitted to this covariance estimate using the ggLASSO Python package with the parameters lambda = 0.1, mu = 100. The result was normalized to obtain an inferred partial correlation matrix, which we use as our phenotype network for downstream analysis.

To cluster the phenotypes, we constructed a weighted *k*-nearest neighbours graph using the absolute partial correlation from above as similarity weights (that is, we retained the *k*-largest weights per node) using $k = 10$. The resulting *k*-nearest neighbours graph was clustered using spectral clustering to obtain 20 clusters, which were labelled by hand. Diet and lifespan were broken out into their own univariate clusters and the body weight cluster was split into lean tissue mass and adiposity (fat mass/total mass) to account for body composition effects known from the literature. This resulted in a summarized representation of 23 clusters (diet, lifespan and 21 groups of traits, one per cluster plus FTM).

We obtained a covariance decomposition by recomputing a sparse low-rank network (as above) on the reduced representation of 23 features. To obtain the relative importance of different effects of DR on lifespan, we performed covariance path decomposition[48] of the covariance between diet and lifespan using this reduced representation graphical model. The absolute values of path scores were used to rank the relative importance of each path and normalized to sum to 1 to estimate the fraction of the covariance between DR and lifespan explained. To obtain network visualizations, the position of nodes and orientation of edges were determined by computing max-flow through the path network. We define the path network as the graph formed by taking the partial correlation network but reweighting edges to be the sum of all (absolute) path scores of paths that contain that edge.

QTL mapping. Genetic mapping analysis of all continuous-valued traits including lifespan was performed using the R package qtl2[63]. Additive covariates for the genome-scan models were diet and body weight variables as indicated in Supplementary Table 5. Founder haplotype effects were estimated treating 8-state genotypes as random effects. Trait heritability was estimated using the R/qtl2 function est.herit() to fit a linear mixed model including an additive kinship matrix. Confidence intervals were obtained by parametric bootstrap. Significance thresholds for QTL mapping were estimated from 1,000 permutations of the trait and covariate data; significant QTL exceed the genome-wide multiple-test adjusted 0.05 threshold (7.5) and suggestive QTL exceed the unadjusted 0.05 threshold (6.0)[64].

Reporting summary

Further information on research design is available in the Nature Portfolio Reporting Summary linked to this article.

Data availability

All processed data, data analysis scripts, supplementary data files and protocols have been deposited at FigShare[65] (https://doi.org/10.6084/m9.figshare.24600255). QTL mapping results can be accessed for download or analysis online (https://churchilllab.jax.org/qtlviewer/DRiDO). Source data are provided with this paper.

Code availability

Scripts written in the R programming language are available to document the analysis of data as reported in the paper and have been deposited at FigShare[65] (https://doi.org/10.6084/m9.figshare.24600255). Scripts used to generate Extended Data Fig. 8 are available at GitHub (https://github.com/calico/DRiDO_Paper_Release).

57. Weindruch, R., Walford, R. L., Fligiel, S. & Guthrie, D. The retardation of aging in mice by dietary restriction: longevity, cancer, immunity and lifetime energy intake. *J. Nutr.* **116**, 641–654 (1986).
58. Smith Jr, D. L. et al. Weight cycling increases longevity compared with sustained obesity in mice. *Obesity* **26**, 1733–1739 (2018).
59. Di Germanio, C., Di Francesco, A., Bernier, M. & de Cabo, R. Yo-Yo dieting is better than none. *Obesity* **26**, 1673 (2018).
60. Lu, Y. J. et al. CD4 T cell help prevents CD8 T cell exhaustion and promotes control of *Mycobacterium tuberculosis* infection. *Cell Rep.* **36**, 109696 (2021).
61. Ingersoll, M. A. et al. Comparison of gene expression profiles between human and mouse monocyte subsets. *Blood* **115**, e10–e19 (2010).
62. Ackert-Bicknell, C. L. et al. Aging research using mouse models. *Curr. Protoc. Mouse Biol.* **5**, 95–133 (2015).
63. Broman, K. W. et al. R/qtl2: software for mapping quantitative trait loci with high-dimensional data and multiparent populations. *Genetics* **211**, 495–502 (2019).
64. Churchill, G. A. & Doerge, R. W. Empirical threshold values for quantitative trait mapping. *Genetics* **138**, 963–971 (1994).
65. Di Francesco, A. et al. Data and code for 'Dietary restriction impacts health and lifespan of genetically diverse mice'. *FigShare* https://doi.org/10.6084/m9.figshare.24600255 (2024).

Acknowledgements We thank the members of the JAX Nathan Shock Center (grant support: NIH P30-038070) Animal and Phenotyping Core team for their assistance with animal husbandry, data collection and curation; the staff at Rockstep for their support with customization of our LIMS system; and G. Ruby for discussions and suggestions; the staff at The Jackson Laboratory's Scientific Services and Center for Biometrics Analysis for expert assistance with the work described in this publication. This work was supported by Calico Life Sciences.

Author contributions A.D.F.: formal analysis, writing, supervision and project administration. A.G.D.: formal analysis and data curation. L.L.: formal analysis and writing. Z.C.: formal analysis and methodology. A.L.: formal analysis and methodology. L.R.: supervision and project administration. G.G.: data collection and data curation. H.D.: data collection and data curation. M.V.: formal analysis. W.S.: data collection and methodology. K.M.W.: formal analysis and methodology. A.R.: formal analysis and methodology. G.V.P.: formal analysis and methodology. M.M.: formal analysis and methodology. W.G.H.: formal analysis and methodology. M.L.Z.: supervision and methodology. L.L.P.: investigation and writing. F.H.: formal analysis, methodology and writing. D.B.: conceptualization and funding acquisition. R.K.: supervision and project administration. C.A.T.: supervision and writing. A.F.: conceptualization, supervision and project administration. G.A.C.: conceptualization, funding acquisition, project administration, formal analysis and writing.

Competing interests A.D.F., Z.C., K.M.W., A.R., G.V.P., M.M., F.H., D.B. and A.F. are employees of Calico Life Sciences. The other authors declare no competing interests.

Additional information

Supplementary information The online version contains supplementary material available at https://doi.org/10.1038/s41586-024-08026-3.

Correspondence and requests for materials should be addressed to Andrea Di Francesco or Gary A. Churchill.

Peer review information *Nature* thanks Johan Auwerx and the other, anonymous, reviewer(s) for their contribution to the peer review of this work. Peer reviewer reports are available.

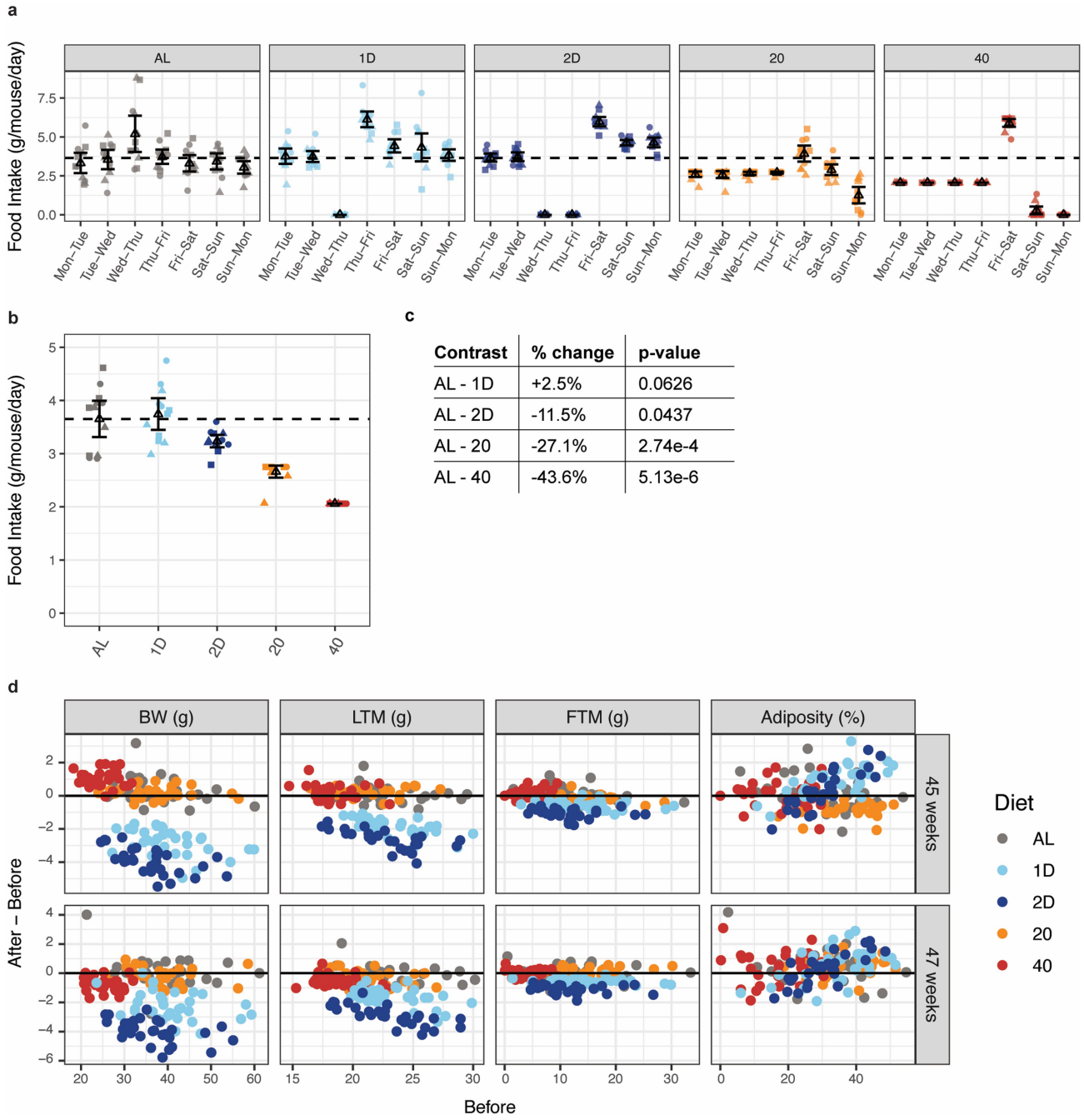

Extended Data Fig. 1 | Food consumption on DR. a, Food consumption was measured for four pens (~ 32 mice) per diet group across three non-consecutive weeks. Daily (3 pm to 3 pm) data shown as average consumption (g/mouse/day) per pen and week of assessment (mean ± 2 s.e.; n = 20 pens). Note that food was refreshed weekly on Wednesday for AL mice. **b**, Cumulative food consumption (g/mouse/day) per pen and week (mean ± 2 s.e.; n = 20 pens). **c**, Cumulative food consumption in each diet group reported as percent change relative to AL. Significance testing of regression coefficients used a 2-sided Wald test. **d**, Changes in body weight (BW), lean tissue mass (LTM), fat tissue mass (FTM), and adiposity at 45 and 47 weeks of age. For IF mice, measurements were taken before and after fasting. For CR mice, measurements were taken before the Friday triple feeding and again before refeeding on Monday. AL mice were assessed on Friday and Monday. Points represent individual mice. On x-axis: before-fasting body weight (g), lean mass (g), fat mass (g), and adiposity (100% x fat mass/total mass). On y axis: difference between before and after, same units.

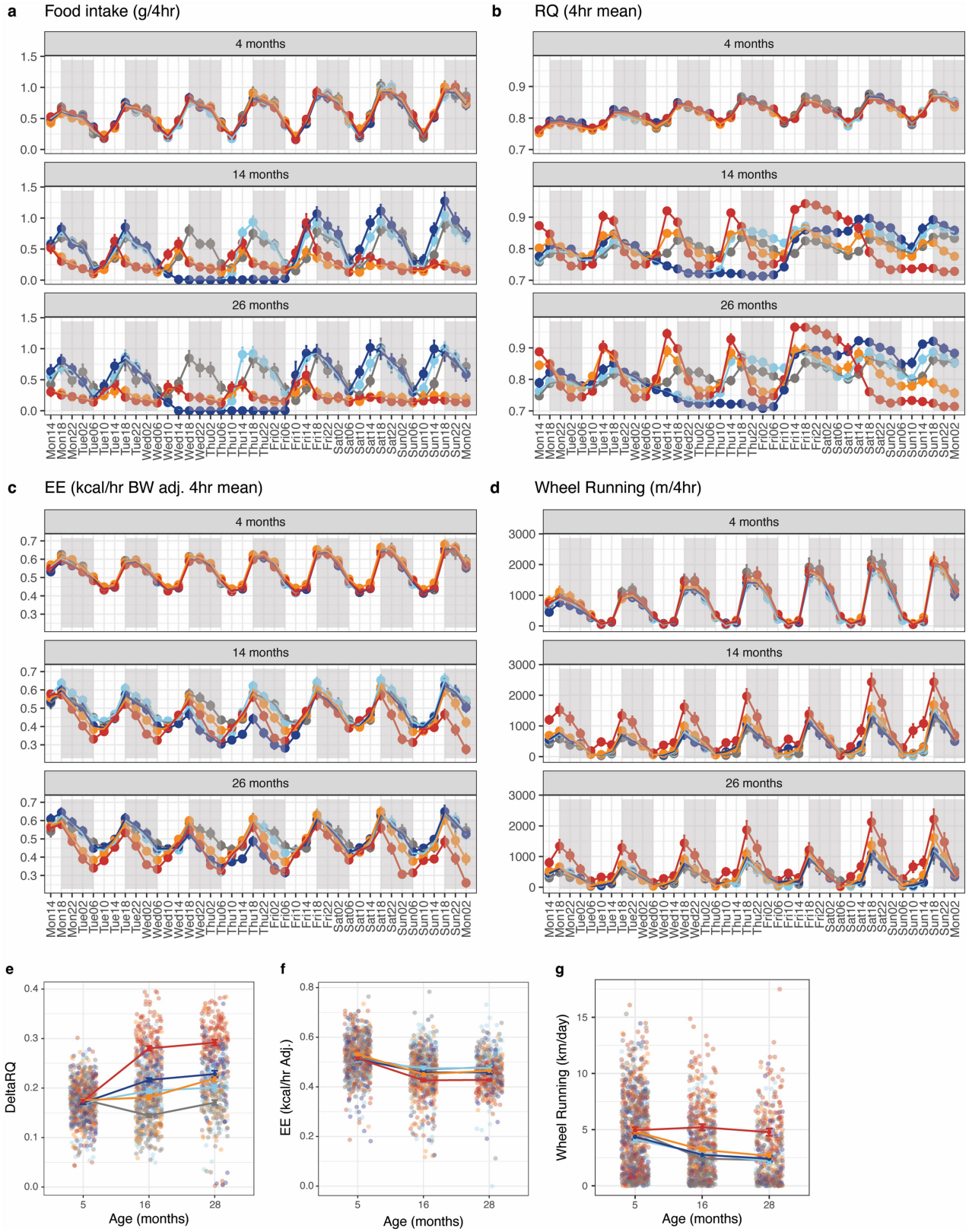

Extended Data Fig. 2 | Metabolic consequences of DR. a, Food consumption from one week of metabolic cage data at ~5, 16, and 28 months of age summarized in 4-hour intervals (mean ± 2 s.e.). x-axis labels represent the start of 4-hour intervals in military time. **b**, Respiratory quotient summarized in 4-hour intervals (mean ± 2 s.e.). **c**, Energy expenditure (kcal per 4 h, adjusted for body weight) summarized in 4-hour intervals (mean ± 2 s.e.). **d**, Distance on running wheel (metres per 4 h) summarized in 4-hour intervals (mean ± 2 s.e.). **e**, Change in respiratory quotient (RQ) (5th to 95th percentile range across one week) showing individuals (points) and averages by diet group and age (mean ± 2 s.e.). **f**, Energy expenditure showing individuals (points) and averages by diet group and age (mean ± 2 s.e.). **g**, Cumulative wheel running (kilometres per day) showing individuals (points) and averages by diet group and age (mean ± 2 s.e.). For all panels **a**-**g** sample sizes are: 5 months n = 889, 16 months n = 760, 28 months n = 528.

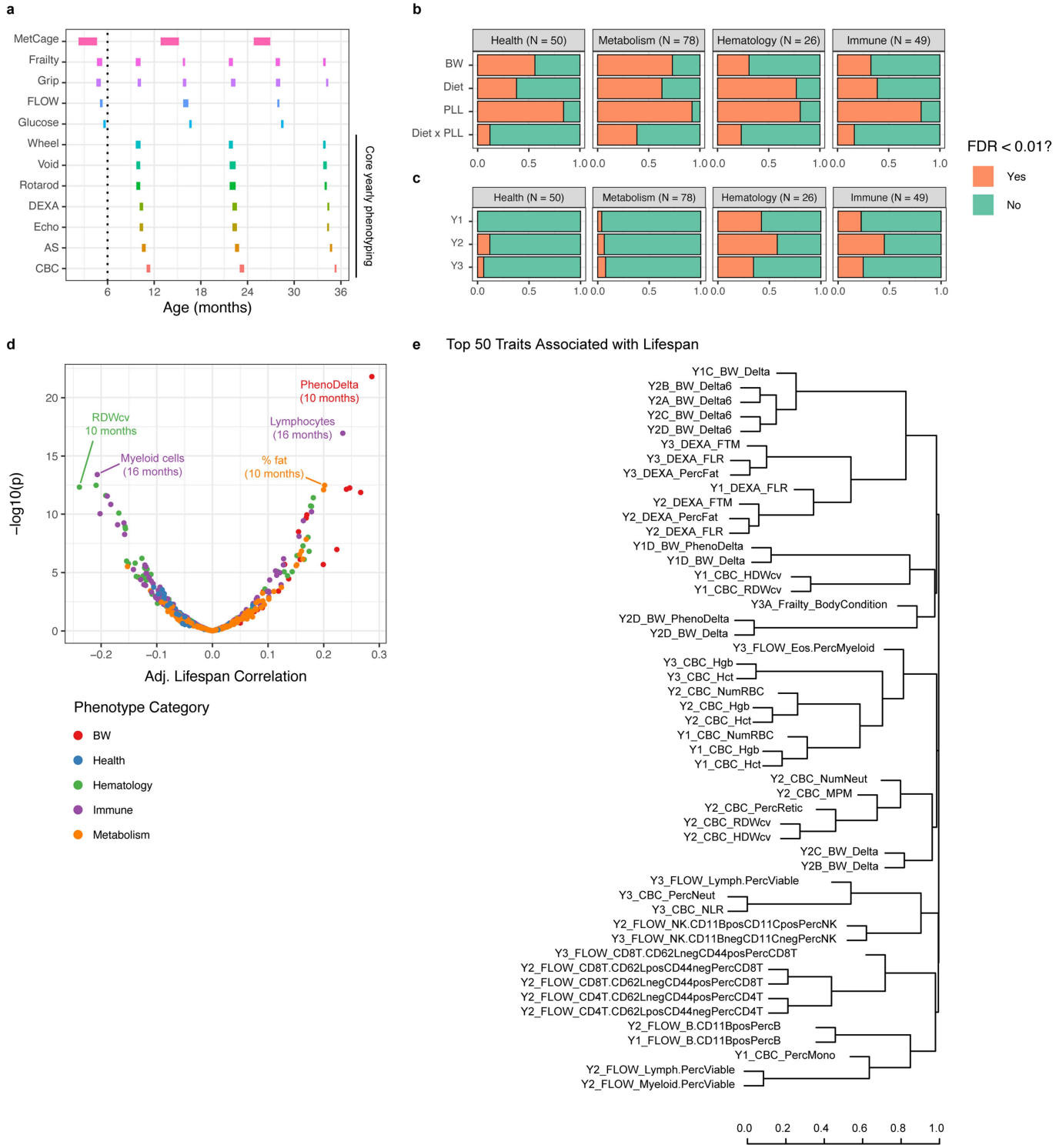

Extended Data Fig. 3 | Statistical analysis of physiological traits. **a**, Overview of the phenotyping schedule: metabolic cages (MetCage), grip strength and frailty exams including body temperature, immune cell profiling by flow cytometry (FLOW), fasted blood glucose, home cage wheel running, voiding assay, rotarod, body composition by dual energy x-ray absorption (DEXA), echocardiogram (Echo), acoustic startle (AS), and complete blood count (CBC). Assays from Wheel to AS constitute the one-month-long intensive phenotyping period. **b**, Barplots showing the number of traits with significant (p^{adj} <0.01) associations with body weight (BW), diet, proportion of life lived (PLL), and diet x PLL interaction. Traits were categorized as health, metabolism, haematology, or immune (see Supplementary Table 6 and **Online Methods**: *Longitudinal Trait Analysis* for statistical test details). **c**, Barplots showing the number of traits that were significantly associated with lifespan after accounting for diet group and body weight. Ages (designated Y1, Y2, Y3) vary depending on the assay (see Supplementary Table 4). For traits with multiple measurements each year, we counted the most significant result (see Supplementary Table 7 and **Online Methods**: *Trait Association with Lifespan* for statistical test details). **d**, Volcano plot showing diet- and BW-adjusted correlations of physiological traits with lifespan vs. statistical significance ($-\log_{10}p$). **e**, Dendrogram shows hierarchical clustering (complete linkage, absolute correlation distance) of 50 traits with the most significant lifespan association. Trait names are shown as Year_AssayType_TraitName as defined in Supplementary Table 5.

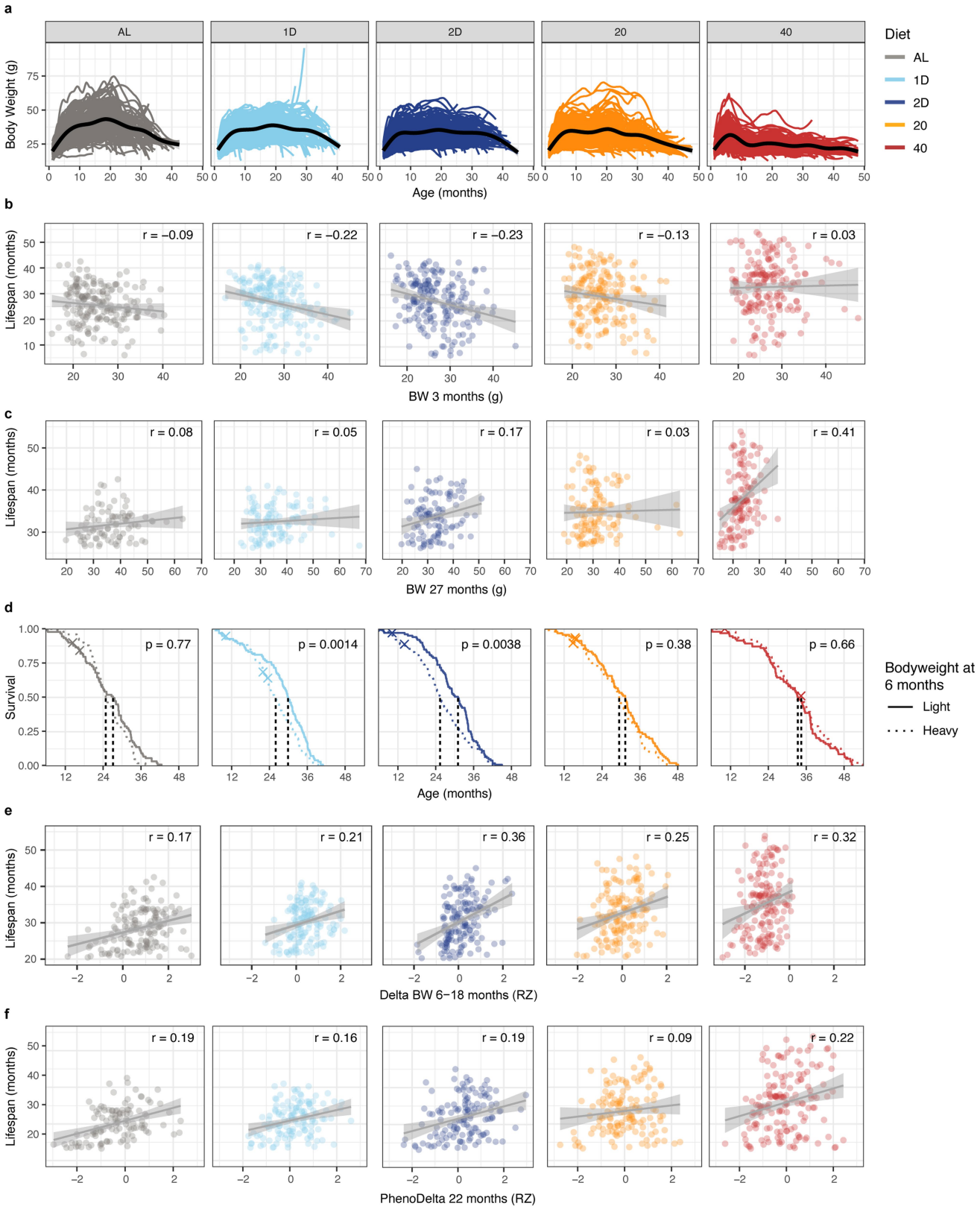

Extended Data Fig. 4 | See next page for caption.

Extended Data Fig. 4 | Body weight traits are associated with lifespan. **a**, Body weight trajectories of individual mice show variation around the loess smoothed mean (black line). **b**, Lifespan by body weight at 3 months (BW, g) with regression line, 95% confidence band, and diet-specific correlations (p^{adj} = 2.48e-4, Diet x Trait:p = 0.0645, r = −0.134). **c**, Lifespan by body weight at 27 months (BW, g) with regression line, 95% confidence band, and diet-specific correlations (p^{adj} = 3.26e-4, Diet x Trait:p = 0.00183, r = 0.137). **d**, Kaplan-Meier curve comparing lifespan for light vs. heavy mice at 6 months of age within each diet group. Statistical significance (p) based on within-diet log rank test comparison of light vs. heavy mice. **e**, Lifespan by change in body weight from 6 to 18 months (Delta BW, RZ = rank normal scores transformed) with regression line, 95% confidence band, and diet-specific correlations (p^{adj} = 5.79e-11, Diet x Trait:p = 0.327, r = 0.266). **f**, Lifespan by change in body weight from 22 to 23 months (PhenoDelta, RZ = rank normal scores transformed) with regression line, 95% confidence band, and diet-specific correlations (p^{adj} =4.07e-9, Diet x Trait:p = 0.530, r = 0.170). See Online Methods: *Trait Association with Lifespan* (panels **b**, **c**, **e**, **f**) for statistical test details.

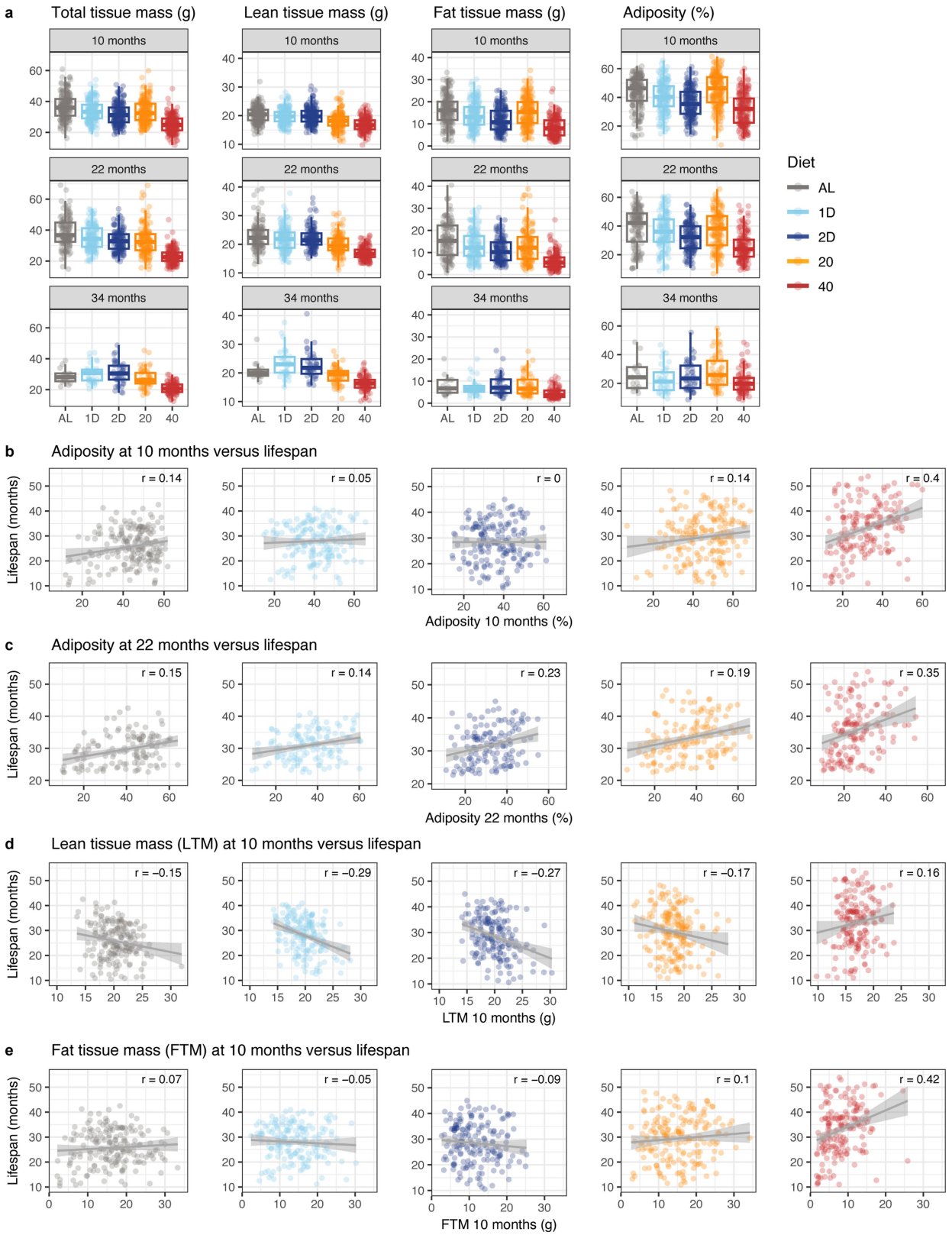

Extended Data Fig. 5 | Body composition traits are associated with lifespan. **a**, Total tissue mass (TTM, g) is decomposed into lean tissue mass (LTM, g), fat tissue mass (FTM, g) and adiposity (100% × FTM/TTM) for individual mice by diet group (colour) and age (10, 22, 34 months). Sample sizes:10 months n = 895, 22 months n = 689, 34 months n = 241 mice. Boxplots show median, quartiles, and range of data. **b**, Lifespan by adiposity at 10 months with regression line, 95% confidence band, and diet-specific correlations (p^{adj} = 3.56e-5, Diet x Trait:p = 0.00230, r = 0.151). **c**, Lifespan by adiposity at 22 months (%) with regression line, 95% confidence band, and diet-specific correlations (p^{adj} = 4.83e-11, Diet x Trait:p = 0.149, r = 0.202). **d**, Lifespan by LTM at 10 months (g) with regression line and diet-specific correlations (p^{adj} = 4.13e-5, Diet x Trait:p^{adj} = 0.0302, r = −0.153). **e**, Lifespan by FTM at 10 months (g) with regression line, 95% confidence band, and diet-specific correlations (p^{adj} = 0.0264, Diet x Trait:p^{adj} = 0.00670, r = 0.0920). See Online Methods: *Trait Association with Lifespan* (panels **b**-**e**) for statistical test details.

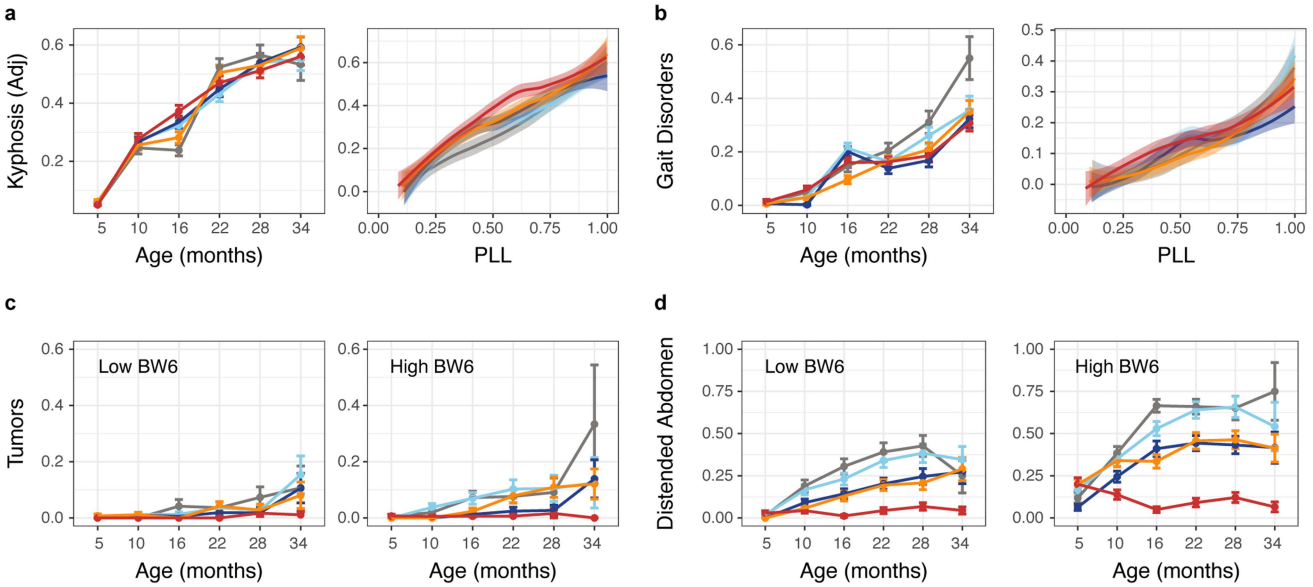

Extended Data Fig. 6 | Health and metabolic traits. a, Kyphosis (scored as 0, 0.5, 1) by age (mean ± 2 s.e.; 5 months n = 770, 10 months n = 909, 16 months n = 834, 22 months n = 704, 28 months n = 489, 34 months n = 260 mice) and by PLL as loess smooth with 95% confidence band (PLL:p < 2.2e-16, Diet:p < 0.00913, Diet x PLL:p = 0.00115). **b**, Gait disorders (scored as 0, 0.5, 1) by age (mean ± 2 s.e.; sample sizes as in panel **a**) and by PLL as loess smooth with 95% confidence band (PLL:p < 2.2e-16, Diet:p < 0.192, Diet x PLL:p = 7.78e-4). **c**, Tumour incidence (scored 0, 0.5, 1) by age (mean ± 2 s.e.; sample sizes as in panel **a**) and stratified by median 6-month body weight. **d**, Distended abdomen incidence (scored 0, 0.5, 1) by age (mean ± 2 s.e.; sample sizes as in panel **a**) and stratified by median 6-month body weight. See Online Methods: *Longitudinal Trait Analysis* (panels **a**-**d**) for statistical test details.

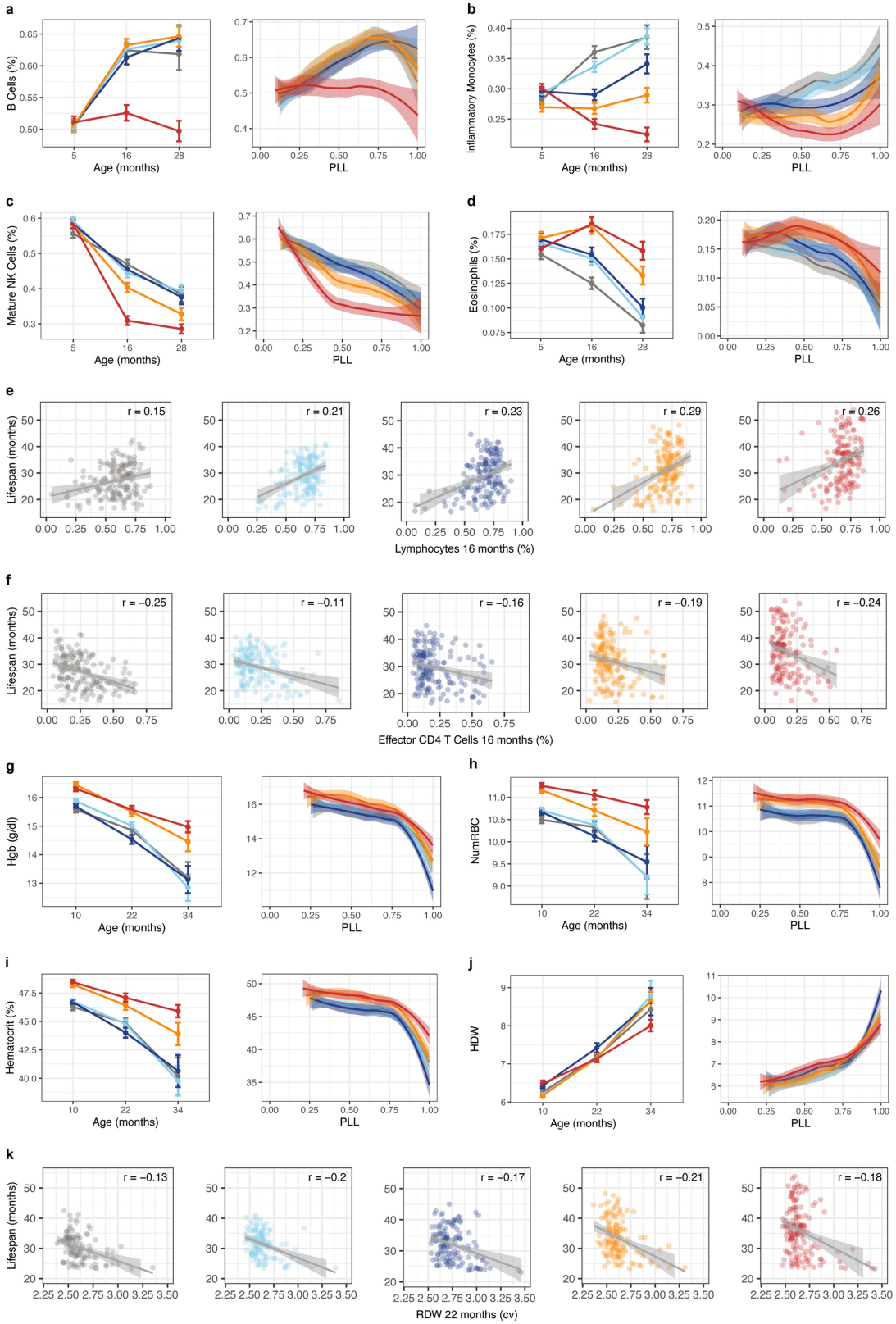

Extended Data Fig. 7 | See next page for caption.

Extended Data Fig. 7 | Immunological and Haematological traits. a, B cells (proportion of lymphocytes) by age (mean ± 2 s.e.; 5 months n = 936, 16 months n = 830, 28 months n = 485 mice) and by PLL as loess smooth with 95% confidence band (PLL:p = 9.85e-8, Diet:p = 2.42e-7, Diet x PLL:p = 0.751). **b**, Inflammatory monocytes (proportion of monocytes) by age (mean ± 2 s.e.; sample sizes as in panel a) and by PLL as loess smooth with 95% confidence band (PLL:p < 1.42e-7, Diet:p < 2.2e-16, Diet x PLL:p = 0.0148). **c**, Mature NK cells (proportion of NK cells) by age (mean ± 2 s.e.; sample sizes as in panel **a**) and by PLL as loess smooth with 95% confidence band (PLL:p < 2.2e-16, Diet:p < 4.08e-7, Diet x PLL:p = 0.0206). **d**, Eosinophils (proportion of myeloid cells) by age (mean ± 2 s.e.; sample sizes as in panel **a**) and by PLL as loess smooth with 95% confidence band (PLL:p < 2.2e-16, Diet:p < 6.93e-7, Diet x PLL:p = 0.210). **e**, Lifespan by Lymphocytes at 16 months (proportion of viable cells) with regression line, 95% confidence band, and diet-specific correlations (p^{adj} = 4.15e-15, Diet x Trait:p = 0.542, r = 0.234). **f**, Lifespan by effector CD4 T cells at 16 months (proportion of CD4 T cells) with regression line, 95% confidence band, and diet-specific correlations (p^{adj} = 1.70e-10, Diet x Trait:p = 0.481, r = −0.189). **g**, Haemoglobin (Hgb, g/dl) by age (mean ± 2 s.e.; 10 months n = 892, 22 months n = 665, 34 months n = 208 mice) and by PLL as loess smooth with 95% confidence band (PLL:p < 2.2e-16, Diet:p < 2.2e-16, Diet x PLL:p = 0.313). **h**, Red blood cell count (NumRBC, 10^6cells/ul) by age (mean ± 2 s.e.; sample sizes as in panel **g**) and by PLL as loess smooth with 95% confidence band (PLL:p < 2.2e-16, Diet:p < 2.2e-16, Diet x PLL:p = 0.999). **i**, Haematocrit (percent red cells) by age (mean ± 2 s.e.; sample sizes as in panel **g**) and by PLL as loess smooth with 95% confidence band (PLL:p < 2.2e-16, Diet:p < 2.2e-16, Diet x PLL:p = 0.508). **j**, Haemoglobin distribution width (HDW, cv) by age (mean ± 2 s.e.; sample sizes as in panel g) and by PLL as loess smooth with 95% confidence band (PLL:p < 2.2e-16, Diet:p = 3.83e-11, Diet x PLL:p = 1.57e-5). **k**, Lifespan by RDW at 22 months (cv) with regression line, 95% confidence band, and diet-specific correlations (p^{adj} = 1.65e-10, Diet x Trait:p = 0.745, r = −0.191). See Online Methods: *Longitudinal Trait Analysis* (panels **a**-**d**, **g**-**j**) and *Trait Association with Lifespan* (panels **e**, **f**, **k**) for statistical test details.

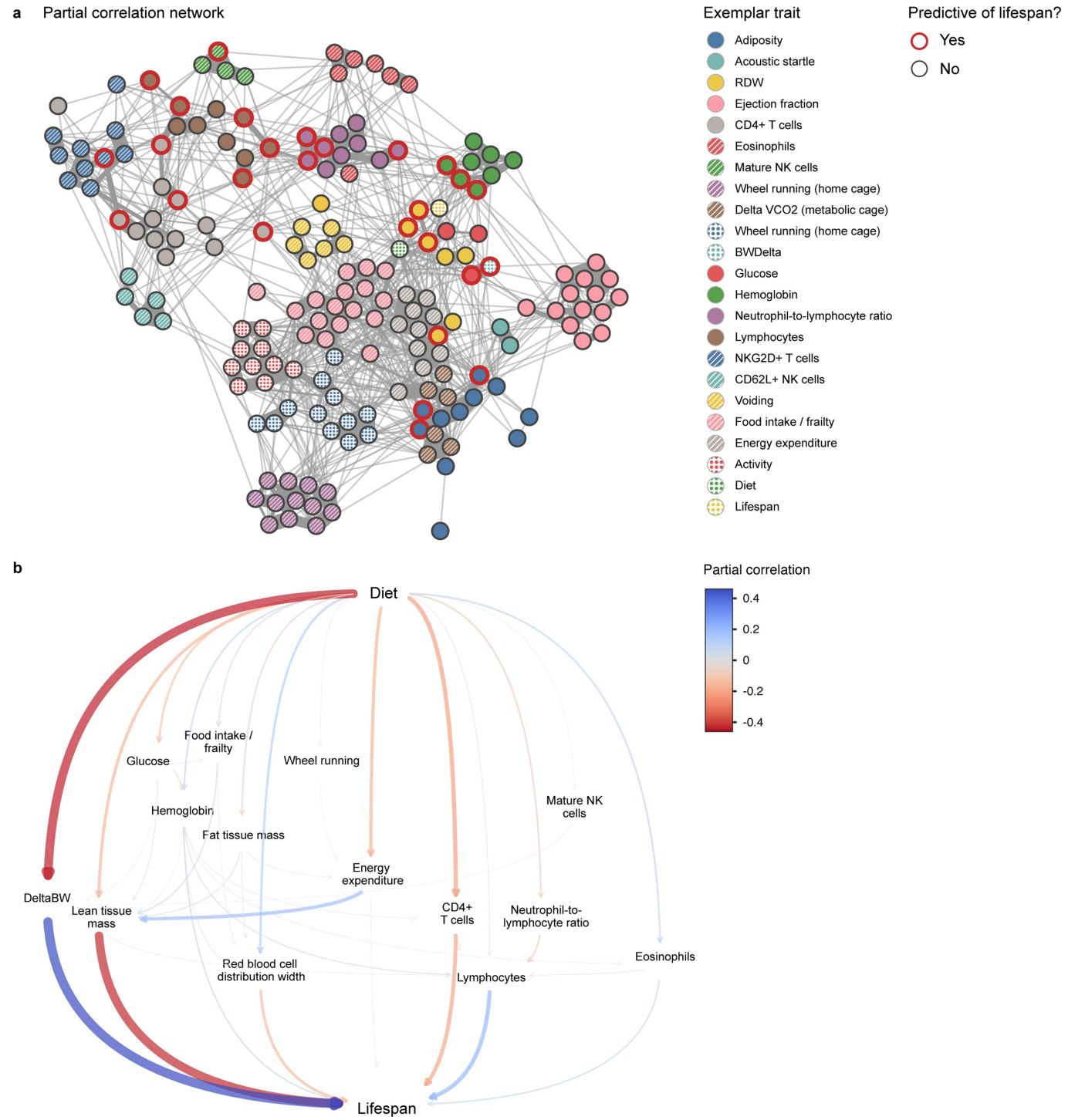

Extended Data Fig. 8 | Multivariate analysis of physiological traits. a, Partial correlation network of 194 traits assayed between 10 and 16 months of age. Trait clusters indicated by colour (see Supplementary Table 10 for details). Points represent individual traits and red outline indicates traits that are significantly associated with lifespan (p^{adj} <0.01). The figure is available as an interactive HTML plot in the FigShare files (see **Data Availability**). Colour key shows the name and age at assessment of the exemplar trait selected to represent each cluster of traits. **b**, Waterfall plot shows the top scoring paths from Diet to Lifespan in the reduced (21 trait) partial correlation network. Size of the arrow is proportional to absolute partial correlation and colour indicates the sign of the partial correlation (colour scale). Abbreviations: Hgb = haemoglobin, LTM = lean tissue mass, FTM = fat tissue mass, RDW = red cell distribution width, NLR = neutrophil to lymphocyte ratio.

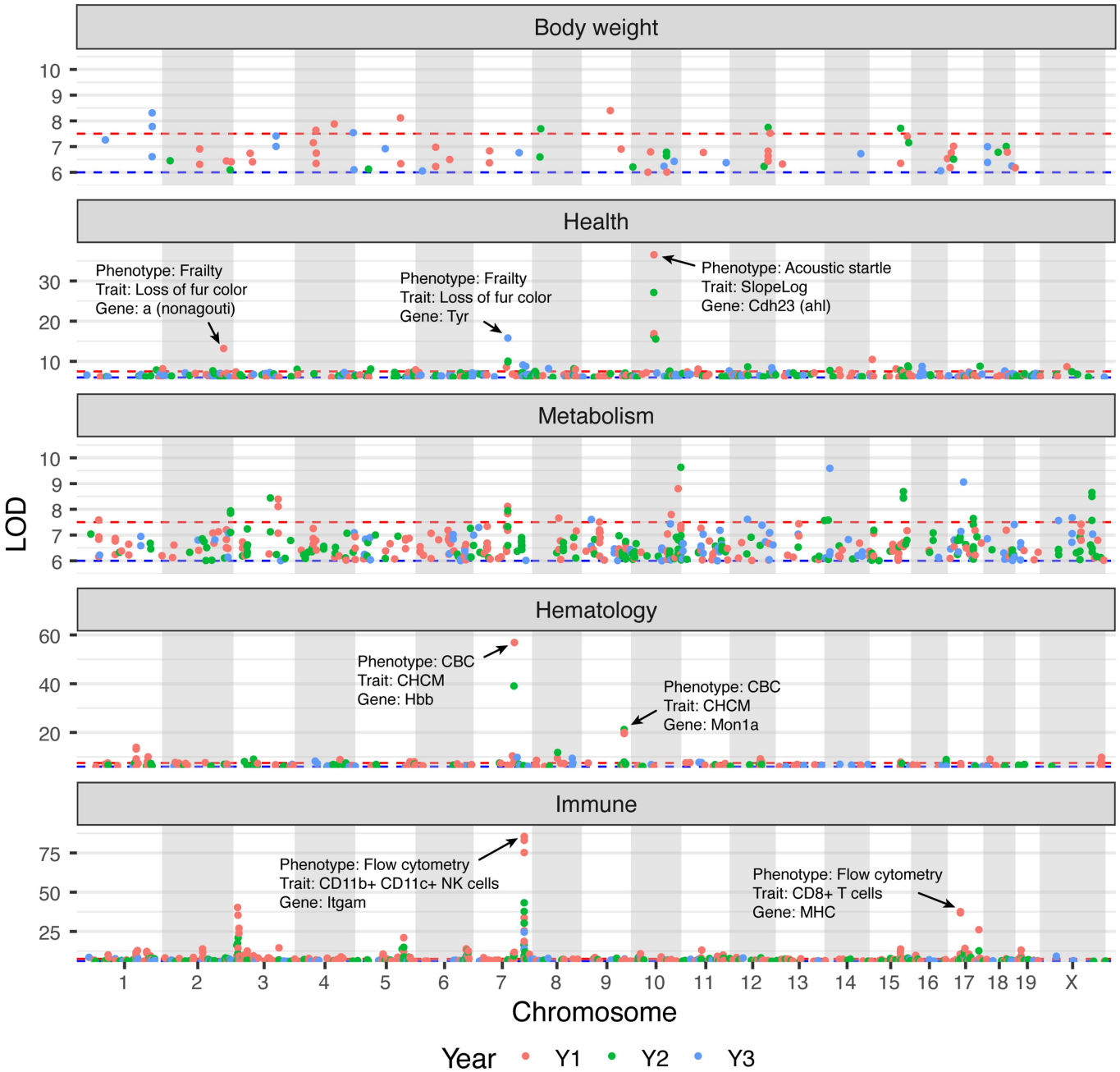

Extended Data Fig. 9 | Genetic mapping of physiological traits. **a**, Manhattan plot shows all LOD peaks above the suggestive threshold (6.0) stratified by domains (facets) and year of assay (colour). Some landmarks include: acoustic startle traits mapped to the age related hearing loss locus (ahl) on chromosome 10 gene *Cdh23*; loss of fur colour (frailty index item) mapped to coat colour genes agouti (*a*) and tyrosinase (*Tyr*) on chromosomes 2 and 7, respectively; haemoglobin traits mapped to the *Hbb* locus on chromosome 7 and *Mon1a* on chromosome 9; NK cell traits mapped to *Itgam* (cell surface marker CD11) on chromosome 7, and additional immune traits mapped to major histocompatibility locus on chromosome 17. Horizontal lines indicate genome-wide adjusted significance thresholds for suggestive (blue) and significant (red, adjusted $p < 0.05$) QTL.

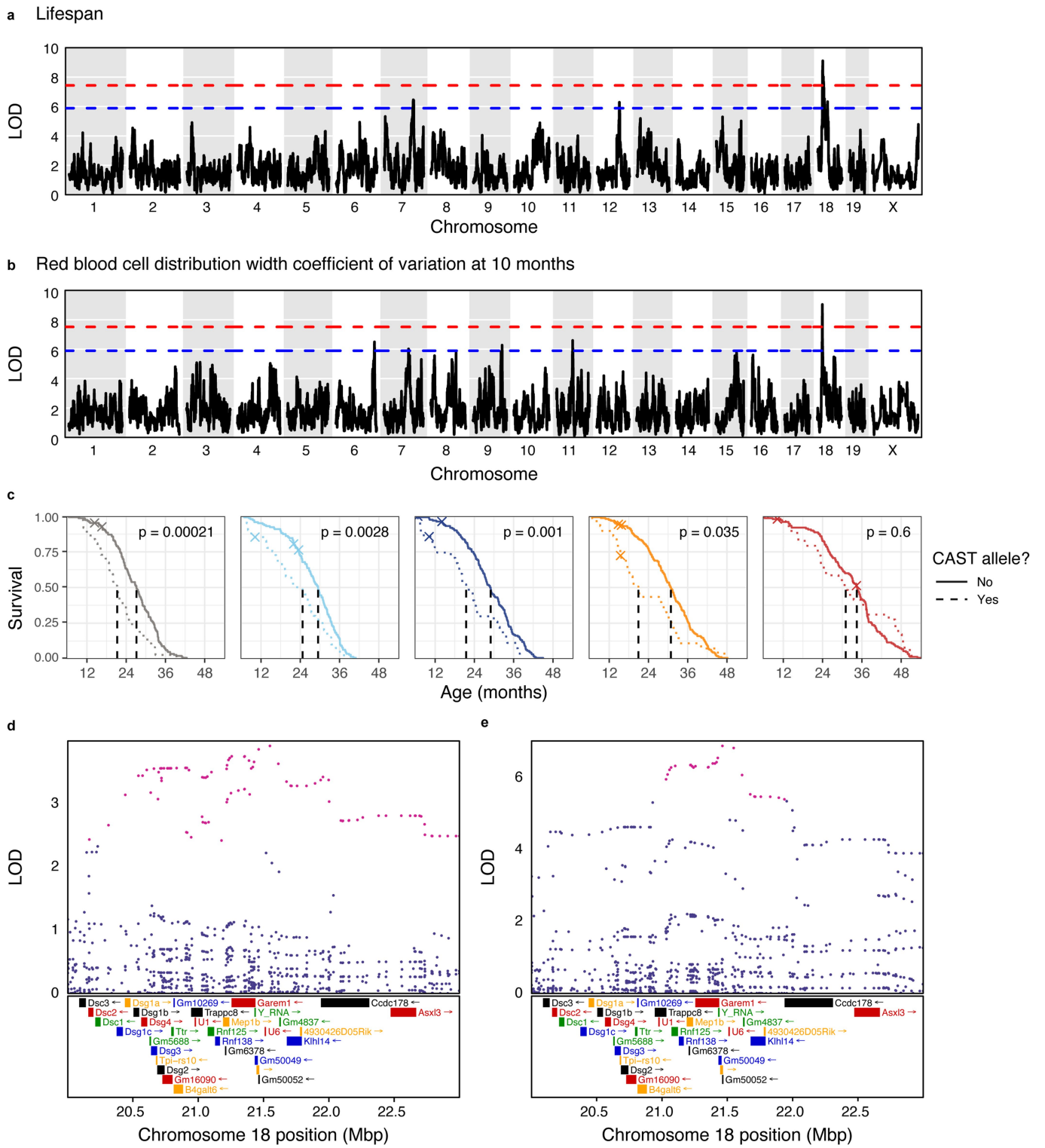

Extended Data Fig. 10 | Genetic mapping of lifespan and RDW. a, Genome-wide QTL mapping of lifespan. Horizontal lines indicate genome-wide adjusted significance thresholds for suggestive (blue) and significant (red, adjusted $p < 0.05$) QTL. **b**, Genome-wide QTL mapping of RDW as in **a**. All panels: x-axis is genomic location (chromosome and position), y-axis is LOD score. **c**, Kaplan-Meier curves within each diet group compare survival of mice stratified by the presence of a CAST allele at the QTL. Statistical significance (p) based on within-diet log rank test comparison of mice with none versus at least one CAST allele at the chromosome 18 QTL peak. **d**, **e**, Association mapping of single nucleotide variants (SNVs) for (**d**) lifespan and (**e**) RDW across the QTL support interval for RDW (21–23 Mb). Chromosomal position is shown on the x-axis, SNV LOD score on the y-axis. SNVs with LOD score with 1.5 units of the top scoring SNV are highlighted (purple). Annotated genes and gene models are shown in their approximate positions below.

nature portfolio

Corresponding author(s): Gary A Churchil

Last updated by author(s): Jun 21, 2024

Reporting Summary

Nature Portfolio wishes to improve the reproducibility of the work that we publish. This form provides structure for consistency and transparency in reporting. For further information on Nature Portfolio policies, see our Editorial Policies and the Editorial Policy Checklist.

Statistics

For all statistical analyses, confirm that the following items are present in the figure legend, table legend, main text, or Methods section.

n/a	Confirmed
☐	☒ The exact sample size (*n*) for each experimental group/condition, given as a discrete number and unit of measurement
☐	☒ A statement on whether measurements were taken from distinct samples or whether the same sample was measured repeatedly
☐	☒ The statistical test(s) used AND whether they are one- or two-sided *Only common tests should be described solely by name; describe more complex techniques in the Methods section.*
☐	☒ A description of all covariates tested
☐	☒ A description of any assumptions or corrections, such as tests of normality and adjustment for multiple comparisons
☐	☒ A full description of the statistical parameters including central tendency (e.g. means) or other basic estimates (e.g. regression coefficient) AND variation (e.g. standard deviation) or associated estimates of uncertainty (e.g. confidence intervals)
☐	☒ For null hypothesis testing, the test statistic (e.g. *F*, *t*, *r*) with confidence intervals, effect sizes, degrees of freedom and *P* value noted *Give P values as exact values whenever suitable.*
☒	☐ For Bayesian analysis, information on the choice of priors and Markov chain Monte Carlo settings
☒	☐ For hierarchical and complex designs, identification of the appropriate level for tests and full reporting of outcomes
☐	☒ Estimates of effect sizes (e.g. Cohen's *d*, Pearson's *r*), indicating how they were calculated

Our web collection on statistics for biologists contains articles on many of the points above.

Software and code

Policy information about availability of computer code

Data collection	n/a
Data analysis	Data analysis was carried out using open source R version 4.4.1 (2024-06-14)

For manuscripts utilizing custom algorithms or software that are central to the research but not yet described in published literature, software must be made available to editors and reviewers. We strongly encourage code deposition in a community repository (e.g. GitHub). See the Nature Portfolio guidelines for submitting code & software for further information.

Data

Policy information about availability of data

All manuscripts must include a data availability statement. This statement should provide the following information, where applicable:

- Accession codes, unique identifiers, or web links for publicly available datasets
- A description of any restrictions on data availability
- For clinical datasets or third party data, please ensure that the statement adheres to our policy

All processed data, data analysis scripts, supplementary data files, and protocols have been deposited with FigShare (https://doi.org/10.6084/m9.figshare.24600255). QTL mapping results can be accessed for download or analysis at https://churchilllab.jax.org/qtlviewer/DRiDO. All processed data, data analysis scripts, supplementary data files, and protocols have been deposited with FigShare (https://doi.org/10.6084/m9.figshare.24600255). QTL mapping results can be accessed for download or analysis at https://churchilllab.jax.org/qtlviewer/DRiDO.

Research involving human participants, their data, or biological material

Policy information about studies with human participants or human data. See also policy information about sex, gender (identity/presentation), and sexual orientation and race, ethnicity and racism.

Reporting on sex and gender	*Use the terms sex (biological attribute) and gender (shaped by social and cultural circumstances) carefully in order to avoid confusing both terms. Indicate if findings apply to only one sex or gender; describe whether sex and gender were considered in study design; whether sex and/or gender was determined based on self-reporting or assigned and methods used.* *Provide in the source data disaggregated sex and gender data, where this information has been collected, and if consent has been obtained for sharing of individual-level data; provide overall numbers in this Reporting Summary. Please state if this information has not been collected.* *Report sex- and gender-based analyses where performed, justify reasons for lack of sex- and gender-based analysis.*
Reporting on race, ethnicity, or other socially relevant groupings	*Please specify the socially constructed or socially relevant categorization variable(s) used in your manuscript and explain why they were used. Please note that such variables should not be used as proxies for other socially constructed/relevant variables (for example, race or ethnicity should not be used as a proxy for socioeconomic status).* *Provide clear definitions of the relevant terms used, how they were provided (by the participants/respondents, the researchers, or third parties), and the method(s) used to classify people into the different categories (e.g. self-report, census or administrative data, social media data, etc.)* *Please provide details about how you controlled for confounding variables in your analyses.*
Population characteristics	*Describe the covariate-relevant population characteristics of the human research participants (e.g. age, genotypic information, past and current diagnosis and treatment categories). If you filled out the behavioural & social sciences study design questions and have nothing to add here, write "See above."*
Recruitment	*Describe how participants were recruited. Outline any potential self-selection bias or other biases that may be present and how these are likely to impact results.*
Ethics oversight	*Identify the organization(s) that approved the study protocol.*

Note that full information on the approval of the study protocol must also be provided in the manuscript.

Field-specific reporting

Please select the one below that is the best fit for your research. If you are not sure, read the appropriate sections before making your selection.

☒ Life sciences ☐ Behavioural & social sciences ☐ Ecological, evolutionary & environmental sciences

For a reference copy of the document with all sections, see nature.com/documents/nr-reporting-summary-flat.pdf

Life sciences study design

All studies must disclose on these points even when the disclosure is negative.

Sample size	Sample size was determined by power calculation to detect 15% change in lifespan with 90% power and type I error < 0.05.
Data exclusions	Mice were randomized to treatments at weaning. Mice that died before 6 months of age (start of treatment) were excluded from analysis,
Replication	Finding are not replicated.
Randomization	Mice were randomized to treatments at weaning using random numbers samples from random.org
Blinding	It was not possible to conduct a blinded study.

Reporting for specific materials, systems and methods

We require information from authors about some types of materials, experimental systems and methods used in many studies. Here, indicate whether each material, system or method listed is relevant to your study. If you are not sure if a list item applies to your research, read the appropriate section before selecting a response.

Materials & experimental systems

n/a	Involved in the study
☐	☒ Antibodies
☒	☐ Eukaryotic cell lines
☒	☐ Palaeontology and archaeology
☐	☒ Animals and other organisms
☒	☐ Clinical data
☒	☐ Dual use research of concern
☒	☐ Plants

Methods

n/a	Involved in the study
☒	☐ ChIP-seq
☒	☐ Flow cytometry
☒	☐ MRI-based neuroimaging

Antibodies

Antibodies used

CD11c FITC, Clone N418, Catalog # 35-0114-U100, Tonbo Biosciences Lot# C0114022619353;
NKG2D (CD314) PE, Clone CX5, Catalog # 558403, BD Biosciences Lot # 8314600;
CD3e PE-CF594, clone 145-2C11, Catalog # 562286 BD Biosciences Lot # 8067789;
CD19 BB700, clone 1D3, Catalog # 566411 BD Biosciences Lot # 1152348;
CD62L PE-Cy7, clone MEL-14, Catalog # 60-0621-U100 Tonbo Biosciences Lot # C0621021418603;
CD25 APC, Clone PC61, Catalog # 102012 Biolegend Lot # B212677;
CD44 APC-Cy7, Clone IM7, Catalog # 25-0441-U100 Tonbo Biosciences Lot # C0441100118253;
Ly6G BV421, Clone 1A8, Catalog # 562737 BD Biosciences Lot # 9162683;
CD4 BV570, Clone RM4-5, Catalog # 100542 Biolegend Lot # B252325;
CD11b BV650, Clone M1/70, Catalog # 563402 BD Biosciences Lot # 6237803;
CD45R/B220 BUV496, Clone RA3-6B2, Catalog # 564662 BD Biosciences Lot # 9085708;
Fc Block, Clone 2.4G2, Cat C247 Leinco Technologies 0622L655

Validation

CD11c FITC: https://cytek-web.s3.amazonaws.com/cytekbio.com/Tonbo/TDS/tds-35-0114.pdf; PMID: 2185332; This antibody preparation has been quality-tested for flow cytometry using mouse spleen cells, or an appropriate cell type.
CD62L PE-Cy7: https://cytek-web.s3.amazonaws.com/cytekbio.com/Tonbo/TDS/tds-60-0621.pdf; PMID: PMID 3084634; This antibody preparation has been quality-tested for flow cytometry using mouse spleen cells, or an appropriate cell type.
CD44 APC-Cy7: https://cytek-web.s3.amazonaws.com/cytekbio.com/Tonbo/TDS/tds-25-0441.pdf; PMID: 11171560; This antibody preparation has been quality-tested for flow cytometry using mouse spleen cells, or an appropriate cell type.
NKG2D (CD314) PE: https://www.bdbiosciences.com/content/dam/bdb/products/global/reagents/flow-cytometry-reagents/research-reagents/single-color-antibodies-ruo/558xxx/5584xx/558403_base/pdf/558403.pdf; PMID: 12370332; The antibody was conjugated with R-PE under optimum conditions, and unconjugated antibody and free PE were removed. The monoclonal antibody was purified from tissue culture supernatant or ascites by affinity chromatography.

CD3e PE-CF594: https://www.bdbiosciences.com/content/dam/bdb/products/global/reagents/flow-cytometry-reagents/research-reagents/single-color-antibodies-ruo/562xxx/5622xx/562286_base/pdf/562286.pdf; PMID: 2470817; The monoclonal antibody was purified from tissue culture supernatant or ascites by affinity chromatography. The antibody was conjugated to the dye under optimum conditions and unconjugated antibody and free dye were removed.

CD19 BB700: https://www.bdbiosciences.com/content/dam/bdb/products/global/reagents/flow-cytometry-reagents/research-reagents/single-color-antibodies-ruo/566xxx/5664xx/566411_base/pdf/566411.pdf; PMID: 9371816; The monoclonal antibody was purified from tissue culture supernatant or ascites by affinity chromatography. The antibody was conjugated with BD HorizonTM BB700 under optimum conditions, and unconjugated antibody and free BD Horizon BB700 were removed.

Ly6G BV421: https://www.bdbiosciences.com/content/dam/bdb/products/global/reagents/flow-cytometry-reagents/research-reagents/single-color-antibodies-ruo/562xxx/5627xx/562737_base/pdf/562737.pdf; PMID: 8360469; The monoclonal antibody was purified from tissue culture supernatant or ascites by affinity chromatography. The antibody was conjugated with BD HorizonTM BV421 under optimum conditions, and unconjugated antibody and free BD HorizonTM BV421 were removed.

CD11b BV650: https://www.bdbiosciences.com/content/dam/bdb/products/global/reagents/flow-cytometry-reagents/research-reagents/single-color-antibodies-ruo/563xxx/5634xx/563402_base/pdf/563402.pdf; PMID: 6184305; The monoclonal antibody was purified from tissue culture supernatant or ascites by affinity chromatography. The antibody was conjugated with BD HorizonTM BV650 under optimum conditions, and unconjugated antibody and free BD HorizonTM BV650 were removed.

CD45R/B220 BUV496: https://www.bdbiosciences.com/content/dam/bdb/products/global/reagents/flow-cytometry-reagents/research-reagents/single-color-antibodies-ruo/612xxx/6129xx/612950_base/pdf/612950.pdf; PMID: 8566073; The monoclonal antibody was purified from tissue culture supernatant or ascites by affinity chromatography. The antibody was conjugated with BD Horizon BUV496 under optimum conditions, and unconjugated antibody and free BD Horizon BUV496 were removed.

CD25 APC: https://www.biolegend.com/en-us/products/apc-anti-mouse-cd25-antibody-420?pdf=true&displayInline=true&leftRightMargin=15&topBottomMargin=15&filename=APC%20anti-mouse%20CD25%20Antibody.pdf&v=20240718123130; PMID: 21347662; Each lot of this antibody is quality control tested by immunofluorescent staining with flow cytometric analysis.

CD4 BV570: https://www.biolegend.com/en-us/products/brilliant-violet-570-anti-mouse-cd4-antibody-7379?pdf=true&displayInline=true&leftRightMargin=15&topBottomMargin=15&filename=Brilliant%20Violet%20570™%20anti-mouse%20CD4%20Antibody.pdf&v=20240718123130; PMID: 20368430; Each lot of this antibody is quality control tested by

immunofluorescent staining with flow cytometric analysis.

Fc Block, Clone 2.4G2: https://www.leinco.com/p/anti-mouse-cd32-cd16-purified-fc-block-antibody/; PMID: 32071068; Leinco antibodies are manufactured in an animal-free facility using only In vitro cell culture techniques and are purified by a multi-step process including the use of protein A or G to assure extremely low levels of endotoxins, leachable protein A or aggregates. Staining of BALB/c splenocytes with Anti-Mouse CD32/16 Purified or Rat IgG1 Isotype Control Purified followed by Goat Anti-Rat IgG (H&L)-FITC.

Animals and other research organisms

Policy information about studies involving animals; ARRIVE guidelines recommended for reporting animal research, and Sex and Gender in Research

Laboratory animals	Outbred mice J:DO
Wild animals	n/a
Reporting on sex	All mice in this study are female. Males were excluded due to potential for agressive behavior as discuss in manuscript.
Field-collected samples	n/a
Ethics oversight	All procedures were reviewed and approved by the Jackson Laboratory Animal Care and Use Comittee

Note that full information on the approval of the study protocol must also be provided in the manuscript.

Plants

Seed stocks	n/a
Novel plant genotypes	n/a
Authentication	n/a